

UNIVERSITY OF TWENTE.

TECHNICAL MEDICINE

---

**The introduction of foetal therapy  
for TTTS patients in the  
Radboudumc**

Including the development of 3D FLOVA-SLAM

---

14<sup>th</sup> September, 2018

*Author:*

C. JELTES

UNIVERSITY OF TWENTE.

TECHNICAL MEDICINE

---

**The introduction of foetal therapy  
for TTTS patients in the  
Radboudumc**

**Including the development of 3D FLOVA-SLAM**

---

14<sup>th</sup> September, 2018

*Author:*

C. JELTES

*Supervisors:*

Prof. Dr. F.P.H.A. Vandenbussche	Head of Obstetrics and Foetal Medicine Obstetrics and Gynaecology - Radboudumc
Dr. Ir. F. van der Heijden	Associate Professor Robotics and Mechatronics - University of Twente
J. Meulstee MSc.	Technical Physician 3D Lab - Radboudumc
Drs. B.J.C.C. Hessink-Sweep	Coordinator Communication & Professional Behaviour University of Twente

# *Preface*

This thesis has been written to fulfil the graduation requirements of the Technical Medicine master program at the University of Twente (UT). I was engaged in researching and writing this thesis from October 2017 to September 2018.

My graduation project started with the question: Can we prevent the common errors during fetoscopic laser coagulation of placental vessels by creating a real-time overview map of the placenta? Already one and a half year ago I started on this project for my third clinical internship. The combination of the medical specialism, the research area and the numerous opportunities, immediately made me feel to continue this research for my graduation internship. By following my own interests for research, education and clinical work, I created myself the perfect graduation project.

The past year a major part of my work was setting up a foetal therapy centre. Together with an amazing and driven team we introduced a very rare and special procedure into the Radboudumc. I feel honoured to be able to work for the foetal therapy team and to provide such special care. Therefore, I would like to thank my medical supervisor Frank Vandenbussche, who initiated this project, who guided me through the year and who gave me so much freedom and responsibility so I could do things I love most. At the beginning of the year I would have never thought to organize demonstrations for medical boards, TV shows our foreign gynaecologists.

Of course I would also like to thank all of the other members of the foetal therapy team, Esther Sikkel, Joris van Drongelen, Mallory Woiski and Sacha Venzelaar-Verhoeven, for their help and enthusiasm for the project. To all my other colleagues at the Obstetrics and Gynaecology department: I would like to thank you for your wonderful cooperation as well.

After leading the project on my own for the first 3 months, I got accompanied by a fellow technical physician Anouk van der Schot by the end of January. Together, we worked on the software that should be able of reconstructing the placenta in 3D during the foetal therapy procedures. Soon we made good progress and were even able to present our work at the Amalia science day. Anouk, I would like to thank you for being my sparring partner, your help, your guidance and of course your company.

Support on the technical aspects of my research was provided by the 3D Lab of the Radboudumc. Therefore, I would like to thank the complete 3D Lab of the Radboudumc. Thereby, I should thank you for the fun time, the enjoying conversations and of course the endless games of table football. In particular, I would like to thank Jene Meulstee, as my technical supervisor inside the Radboudumc, you were always available for instant feedback. You kept an eye on the progress of the project and helped showing me that there is more than just one kind of technical physician.

I also want to thank my supervisors at the UT. Ferdi van der Heijden, thank you for your guidance on the technical aspects of my research. Bregje Hessink-Sweep, thank you for your guidance on my process and my personal growth the past two years. Maybe this personal development was my biggest achievement of this year.

Last but not least, I would like to thank my friends, family and boyfriend! If I ever lost my motivation, got overwhelmed by stress our thought about it would never be good enough: your words made me trough.

At the end of this graduation year, I can conclude that I have learned a lot about the twin-twin transfusion syndrome, foetal therapy and simultaneously localization and mapping. Moreover, I learned to cooperate with many different disciplines, to organize trainings, to present myself to others and to demonstrate my work. However, there is still more to learn and therefore I am excited to continue working within this amazing team and research project.

I hope you all enjoy reading this thesis.

Claire Jeltens

Nijmegen, September 14, 2018

# *Table of contents*

<b>Abstract</b>	<b>1</b>
<b>List of Abbreviations</b>	<b>1</b>
<b>1 General Introduction</b>	<b>3</b>
1.1 Invasive Foetal Therapy Centre . . . . .	4
1.2 3D Placenta Reconstruction . . . . .	4
1.3 Thesis Outline . . . . .	5
<b>2 Background</b>	<b>7</b>
2.1 Twin-twin Transfusion Syndrome . . . . .	8
2.2 Fetoscopic Laser Coagulation . . . . .	11
<b>3 Introducing Fetoscopic Laser Occlusion of Vascular Anastomoses in the Radboudumc</b>	<b>15</b>
3.1 Introduction . . . . .	16
3.2 Infrastructure and Materials . . . . .	17
3.3 Procedures and Protocols . . . . .	20
3.4 Monitoring and Reporting . . . . .	23
3.5 Training and Schooling . . . . .	27
3.6 Discussion . . . . .	30
3.7 Conclusion . . . . .	31

<b>4</b>	<b>3D Reconstruction of Fetoscopic Videos for Artificial Field of View Expansion during Foetal Surgery</b>	<b>33</b>
4.1	Introduction . . . . .	34
4.2	3D FLOVA-SLAM . . . . .	36
4.3	Image Acquisition . . . . .	38
4.4	Camera Calibration . . . . .	42
4.5	Feature Extraction . . . . .	50
4.6	3D Reconstruction . . . . .	59
4.7	Texture Reconstruction . . . . .	66
4.8	Discussion . . . . .	70
4.9	Conclusion . . . . .	72
<b>5</b>	<b>Conclusions and Recommendations</b>	<b>73</b>
<b>6</b>	<b>Appendices</b>	<b>83</b>
6.1	Appendix A: Calibration Protocol . . . . .	84
6.2	Appendix B: Calibration Method . . . . .	86
6.3	Appendix C: ORB Feature Extraction . . . . .	88
6.4	Appendix D: ORB-SLAM . . . . .	90

---

## Abstract

The twin-twin transfusion syndrome (TTTS) occurs in 20% of the monochorionic pregnancies and results from unbalanced foeto-foetal blood transfusion between the donor twin and the recipient twin through placental anastomoses. Fetoscopic laser occlusion of vascular anastomoses (FLOVA) is commonly used to treat the underlying pathology of TTTS. During this procedure the anastomoses are identified and coagulated using a small fetoscope. In this way the two foetal circulations will become separated and blood transfusions cannot longer occur. In the Netherlands the referral hospital for patients with TTTS is the Leiden University Medical Center (LUMC). Although, FLOVA is commonly used in the field of foetal therapy, it is characterized by the disadvantage of a small field of view during the procedure. This can lead to a difficulty in orientation and navigation for the surgeon.

The first objective of this research was to implement FLOVA in the Radboudumc and to create the second invasive foetal therapy centre of the Netherlands. The second aim of this project was to overcome the problems of the limited field of view during FLOVA by implementing a method that can provide a real-time 3D overview map of the placental vascular topography. This map can help the surgeon orientate and navigate during the FLOVA procedures, potentially improving the accuracy and thereby reducing the chance of complications, the operation time and the costs.

Years of preparation, were followed by the introduction of the FLOVA procedure in the Radboudumc in January this year. Hereby, the Radboud now is the referral centre for the eastern part of the Netherlands. In May the first FLOVA operation was successfully performed. Furthermore, a framework for the 3D FLOVA-SLAM software has been developed. 3D FLOVA-SLAM is based on the recently developed ORB-SLAM and is used to generate a real-time textured 3D reconstruction of the placenta. The 3D FLOVA-SLAM method can be used without external hardware. The first results of using 3D FLOVA-SLAM on placental videos are promising, indicating that our approach has a high chance of success to address the urgent problem of the limited field of view during FLOVA procedures.

The hypothesis is that, with the real-time map of the placenta, surgeons can use smaller diameter instruments during the procedure and hereby reduce the associated risks and complications, like pregnancy loss. Furthermore, we expect that a better orientation for the surgeon will lead to a faster procedure, shorter learning curves and improved accuracy leading to lower risk of complications.

---

## List of abbreviations

3D	3-Dimensional
BRIEF	Binary Robust Independent Elementary Features
CCMO	Central Committee on Human Research
DRE	Digital Research Environment
EKF	Extended Kalman Filter
ECMO	Extracorporeal Membrane Oxygenation
EM	Electromagnetic
FAST	Features from Accelerated Segment Test
FETO	Fetoscopic Endoluminal Tracheal Occlusion
FLOC	Fetoscopic Laser Occlusion of Chorioangiopagous vessels
FLOVA	Fetoscopic Laser Occlusion of Vascular Anastomosis
IFTC	Invasive Foetal Therapy Centre
IUFD	Intrauterine Foetal Demise
IUGR	Intrauterine Growth Restriction
LUMC	Leids University Medical Centre
MVP	Maximum Vertical Pocket
NICU	Neonatal Intensive Care Unit
NVOG	Dutch society for Obstetrics and Gynaecology
ORB	Orientated FAST and rotated BRIEF
(i)PPROM	(iatrogenic) Preterm Pre-labour Rupture Of Membranes
PTAM	Parallel Tracking and Mapping
Radboudumc	Radboud University Medical Centre
RANSAC	Random Sample Consensus
RCT	Randomized Controlled Trial
rTTTS	recurrent Twin-Twin Transfusion Syndrome
SfM	Structure from Motion
SIFT	Scale Invariant Feature Transform
SLAM	Simultaneous Localization And Mapping
SLCPV	Selective Laser Coagulation of Placental Vessels
SQLCPV	Sequential Selective Laser Coagulation of Placental Vessels
SURF	Speeded Up Robust Features
TAPS	Twin Anaemia Polycythaemia Sequence
TOPS	Twin Oligohydramnios-Polyhydramnios Sequence
TTTS	Twin-Twin Transfusion Syndrome
URS	Uretero-Renoscope

# Chapter 1

---

## *General Introduction*

1.1	Invasive Foetal Therapy Centre . . . . .	4
1.2	3D Placenta Reconstruction . . . . .	4
1.3	Thesis Outline . . . . .	5

---

## 1.1 Invasive Foetal Therapy Centre

Since 2011, the Radboud University Medical Centre (Radboudumc) has the ambition to become an Invasive Foetal Therapy Centre (IFTC) focusing on both Fetoscopic Laser Occlusion of Vascular Anastomosis (FLOVA) and Fetoscopic Endoluminal Tracheal Occlusion (FETO). Setting up a foetal therapy centre follows logically from the ambitions and capabilities of the Radboudumc. The Radboudumc is an important tertiary care centre for perinatology and paediatrics. Furthermore, it has employed an experienced gynaecologist in maternal-foetal medicine and foetal therapy. In addition, the Radboudumc houses a Neonatal Intensive Care Unit (NICU) in combination with a department for paediatric surgery and the possibility to provide Extracorporeal Membrane Oxygenation (ECMO), which is required for FETO treatment.

Worldwide around 100 hospitals participate in foetal therapy care. In the Netherlands only one centre performs foetal surgeries, the Leiden University Medical Center (LUMC). The LUMC performs around 60 ultrasound guided needle procedures and 85 fetoscopic operations per year, mainly focussing on foetal blood transfusion and FLOVA operations<sup>1</sup>. The Radboudumc aims at becoming the referral foetal therapy centre for the eastern part of the Netherlands. This could potentially lead to better outcomes since it overcomes the disadvantages of a care monopoly<sup>2</sup>. Moreover, it improves the patient comfort by reducing the distance to care. In addition, timely referral improves the foetal outcome<sup>3</sup>.

Due to the technical challenging nature of foetal therapy, a widespread could lead to less favourable outcomes through the 'learning curve effect'<sup>4,5</sup>. For this reason much care and effort were put into the implementation process of foetal therapy in the Radboudumc. The quality norm on invasive foetal therapy of the Dutch society for Obstetrics and Gynaecology (NVOG) was used as a guideline for the implementation<sup>1</sup>.

## 1.2 3D Placenta Reconstruction

In addition to the implementation of standard foetal therapy care in the Radboudumc, innovative ways to improve the procedure and outcomes of foetal surgery are implemented. FLOVA operations are associated with a high risk of complications, such as (iatrogenic) Preterm Pre-labour Rupture Of Membranes (iPPROM)<sup>6</sup>. We have developed a technique that could potentially reduce these risks. 3D Placenta reconstruction software was created in order to produce a real-time map of the placenta and amniotic cavity environment. This map can help

---

the surgeon orientate and navigate during foetal therapy proceedings. Potentially improving the accuracy and thereby reducing the chance of complications, the operation time and the costs.

## 1.3 Thesis Outline

This report documents on both the process of implementing foetal therapy in the Radboudumc, and on the innovative method to improve the outcomes of FLOVA surgery. The report is divided into 5 sections. After this introduction and problem formulation, chapter 2 provides a description of both TTTS and FLOVA. In chapter 3, the complete implementation process of the FLOVA operation is described. Chapter 4 gives a detailed description of the innovative method that was designed to overcome the risks and complications of FLOVA. In chapter 5 the most important recommendations for the future are elaborated.



# Chapter 2

---

## *Background*

2.1	Twin-twin Transfusion Syndrome . . .	8
2.2	Fetoscopic Laser Coagulation . . . . .	11

---

## 2.1 Twin-twin Transfusion Syndrome

Monochorionic twin pregnancies are associated with a high risk for perinatal complications like the twin-twin transfusion syndrome (TTTS)<sup>7,8</sup>. TTTS results from unbalanced foetofetal blood transfusion between the donor twin and the recipient twin through intertwin placental anastomoses, illustrated in figure 2.1<sup>9,10</sup>. TTTS occurs in 8-10% of the monochorionic pregnancies.<sup>11,12,13</sup> Without treatment TTTS results in prenatal death for both twins in up to 90% of the cases<sup>14,15</sup>. In addition, high rates of impaired neurological development are seen in survivors<sup>13,16</sup>.

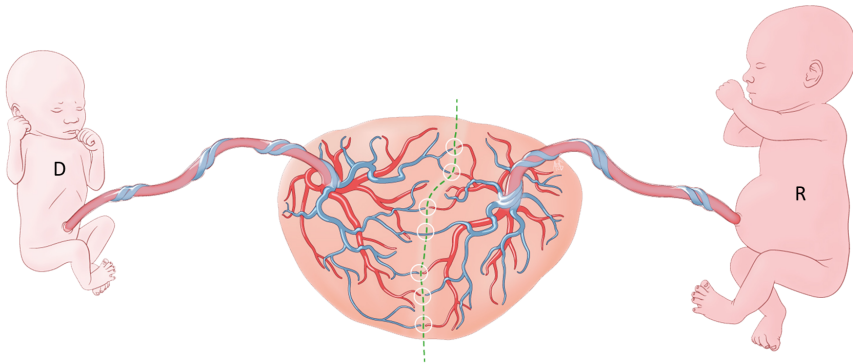


**Figure 2.1 Schematic illustration of the twin-twin transfusion syndrome.** The green line indicates the vascular equator. The white circles indicate several anastomosis. The donor (D) twin is illustrated on the left, the recipient (R) twin on the right.<sup>17</sup>

### 2.1.1 Pathophysiology

The unbalanced foetofetal blood transfusion between twins is created by vascular anastomosis along a vascular equator. The anastomoses can be of different types: artery-to-vein (AV), artery-to-artery (AA) or vein-to-vein (VV). Most anastomosis are deep AV anastomoses through a shared placental cotyledon. AV anastomosis in opposite direction and AA anastomoses are believed to have a compensatory effect on the blood transfusion from donor to recipient.<sup>10,18,19</sup>

The unbalanced blood transfusion results in hypervolemia of the recipient and hypovolemia of the donor. In this way the donor twin becomes oliguric or anuric and the recipient twin becomes polyuric. Oligohydramnios develops in the amniotic sac of the donor twin and polyhydramnios in the amniotic sac of the recipient twin (figure 2.2).<sup>10,18,19</sup>

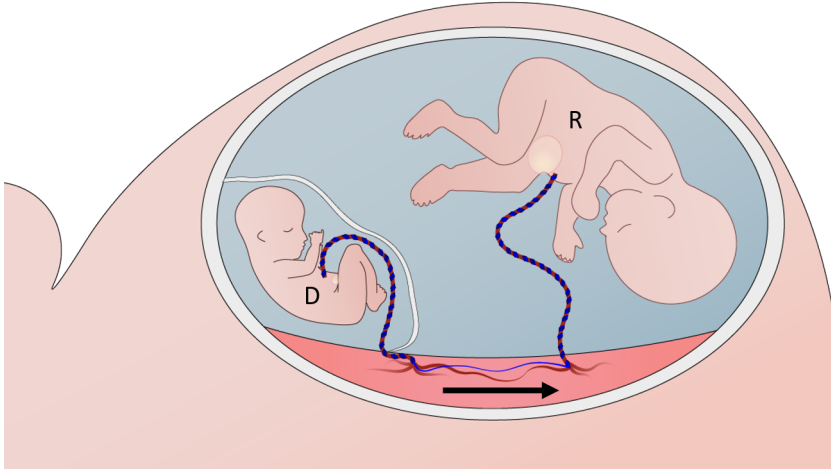


**Figure 2.2 Schematic illustration of the twin-twin transfusion syndrome.** The syndrome is characterized by a combination of oligohydramnios in the donor (D) twin and polyhydramnios in the recipient (R) twin. This leads to a large bladder in the recipient twin and a small bladder in the donor twin. TTTS arises due to the net foetofoetal (arrow) blood flow in the direction of the recipient.

### 2.1.2 Diagnosis

TTTS is usually diagnosed during a routine ultrasound follow-up of an asymptomatic monochorionic pregnancy (figure 2.3). The most important diagnostic criterion for TTTS is Twin Oligohydramnios-Polyhydramnios Sequence (TOPS), defined as the combination of oligohydramnios (Maximum Vertical Pocket (MVP) in amniotic sac  $\leq 2$  cm) in one twin and polyhydramnios in the other twin (MVP  $\geq 8$  cm)<sup>9,20,21</sup>. Furthermore, frequent symptoms of the donor twin are Intrauterine Growth Restriction (IUGR) and a small or even absent bladder. On the other hand, the recipient twin is characterized by a distended bladder and in some cases TTTS-related cardiopulmonary problems such as right ventricular outflow tract obstruction<sup>10</sup>. Less frequently, the diagnosis of TTTS may be suspected based on acute clinical symptoms related to polyhydramnios, such as uterine distension, contractions, or maternal dyspnea.<sup>9,10,20</sup>

Staging of TTTS can be performed with the Quintero classification system, which stratifies TTTS into 5 stages (table 2.1). The staging is based on the ultrasound results in combination with Doppler studies on the umbilical artery, umbilical vein and ductus venosus of both twins.<sup>20,21</sup>

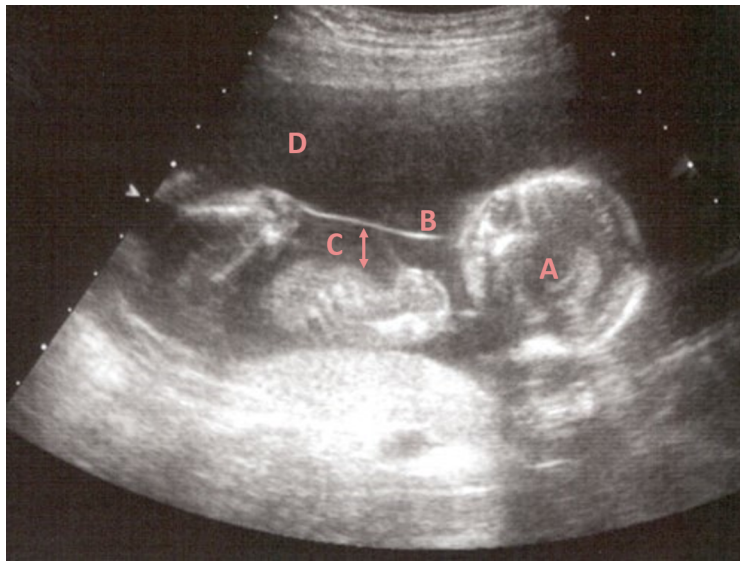


**Figure 2.3** Ultrasound image of a donor twin affected with the twin-twin transfusion syndrome. (a) The donor twin stuck in his amniotic sac, (b) the intertwin membrane, (c) the Maximum Vertical Pocket (MVP), (d) polyhydramnios in the amniotic sac of the recipient twin.

**Table 2.1** The Quintero classification system.<sup>20</sup>

Stage	Classification
I	There is a discrepancy in amniotic fluid volume with oligohydramnios of a maximum vertical pocket (MVP) $\leq 2$ cm in one sac and polyhydramnios in other sac (MVP $\geq 8$ cm). The bladder of the donor twin is visible and Doppler studies are normal.
II	The bladder of the donor twin is not visible (during length of examination, usually around 1 hour) but Doppler studies are not critically abnormal.
III	Doppler studies are critically abnormal in either twin and are characterized as abnormal or reversed end-diastolic velocities in the umbilical artery, reverse flow in the ductus venosus or pulsatile umbilical venous flow.
IV	Ascites, pericardial or pleural effusion, scalp oedema or overt hydrops present.
V	One or both babies are dead.

### 2.1.3 Treatment

Without treatment, TTTS is associated with extremely high mortality rates up to 90%<sup>14,15</sup>. Treatment options to overcome the symptoms of TTTS include: serial amnioreduction, amniotic septostomy, elective preterm delivery, selective reduction of one fetus or termination of the pregnancy<sup>9,21</sup>. Serial amnioreduction

---

improves the outcomes of TTTS, but is still associated with 60% mortality and 50% severe neurodevelopment impairment<sup>22</sup>. In contrast to symptom-fighting treatments, FLOVA, also called fetoscopic laser coagulation of communicating vessels (FLOC), can be used to treat the underlying pathology<sup>9,23</sup>.

## 2.2 Fetoscopic Laser Coagulation

Since 2004, FLOVA is the treatment of choice for TTTS (figure 2.4). In the Euro-fetus trial Senat et al. proved that FLOVA results in higher survival rates (76% vs. 56% survival of at least one twin) as compared with serial amnioreduction. Furthermore, patients treated with FLOVA were more likely to be free of neurological complications, like intra-ventricular haemorrhage and blindness, at six months of age (52 % vs. 31 %).<sup>23</sup>

### 2.2.1 History

In 1990, De Lia et al. published his method to fetoscopically coagulate the vascular anastomosis causing TTTS<sup>24</sup>. During the procedure, all vessels crossing the inter-twin membrane were coagulated resulting in two separated blood circulations. The anastomoses are coagulated using a Nd:YAG or diode laser with an optimal energy absorbency in the spectrum of haemoglobin.<sup>25</sup> This method significantly improved the survival rates of twins with TTTS by treating the underlying pathology of TTTS. However, high mortality rates of 20-48% were still seen.<sup>6,24,26</sup>

### The Selective Laser Coagulation Technique

In 1998, Quintero et al. introduced, the Selective Laser Coagulation of Placental Vessels technique (SLCPV), an improved method in which only true inter-twin anastomoses were coagulated instead of all vessels crossing the membranous equator<sup>27</sup>. Hereby, the functioning placenta tissue is spared as much as possible. Quintero et al. found a higher survival rate of at least one twin in the selective laser coagulation group (83.1% vs. 61.1%), mainly caused by a lower incidence of Intrauterine Foetal Demise (IUFD)<sup>28</sup>.

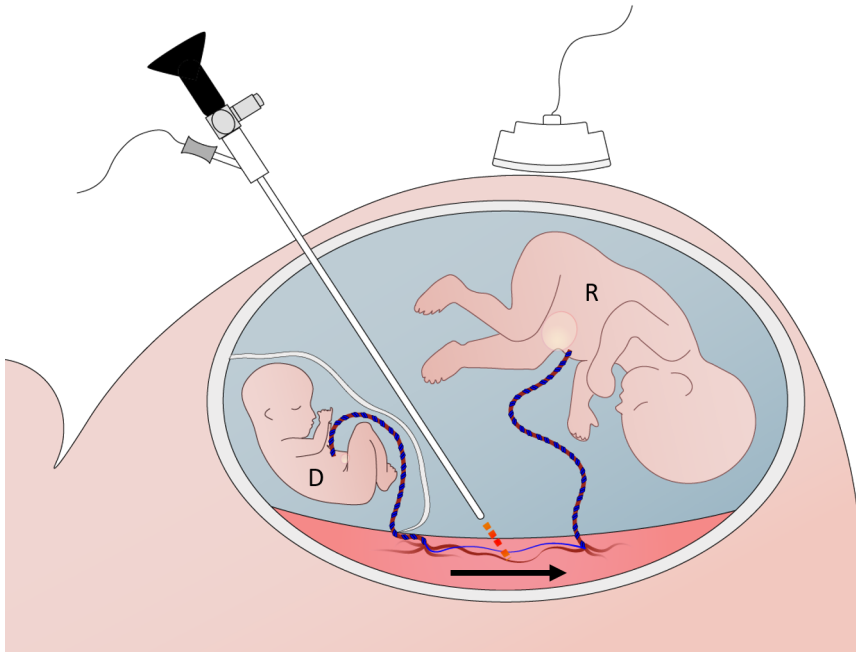


**Figure 2.4 Schematic illustration of the fetoscopic laser occlusion of vascular anastomoses.** A fetoscope is entered into the uterus under constant ultrasound guidance. The polyhydramnios in the recipient twin (R) amniotic sac provides the surgeon with a view on the vascular equator. All anastomoses are identified and coagulated using a laser.<sup>31</sup>

### The Sequential Selective Laser Coagulation Technique

In 2007, Quintero et al. proposed the Sequential Selective Laser Coagulation of Placental Vessels technique (SQLCPV), which aims to avoid intraoperative shifts in the blood transfusion by coagulating the anastomoses in a specific order<sup>29</sup>. The AV anastomoses are coagulated first, followed by the compensating VA anastomoses and finally the AA or VV anastomoses. The SQLCPV method allows decompression of the recipient vascular overload before the separation is complete, possibly resulting in better (neurological) outcomes. Gemert et al. proved this theory by analysing a mathematical model of pressure gradients, flow and resistance<sup>30</sup>.

---

## The Solomon Technique

In 2014, Slaghekke et al. published the SOLOMON trial in which they conclude that the newly developed Solomon laser technique reduces postoperative foetal morbidity<sup>32</sup>. The Solomon procedure always follows after the SLCPV or SQLCPV technique and aims at a complete dichorionization of the placenta by coagulating the entire vascular equator. In practice, the surgeon connects all laser spots by drawing a laser line from one side of the placenta to the other. Slaghekke et al. concluded that the risk of Twin Anemia Polycythemia Sequence (TAPS) (from 16% to 3%) and recurrent TTTS (from 7% to 1%) reduces with the use of the Solomon technique<sup>32</sup>.

### 2.2.2 Current Situation

The survival rate of monochorionic twins treated with FLOVA significantly improved since the introduction in 1990<sup>33</sup>. Due to better surgery techniques, more awareness for TTTS and the 'learning curve effect' the survival of both fetuses improved from 31% (1990-1995) to 62% (2011-2014) and for one foetus from 70% to 88%<sup>33</sup>. Diehl et al. recently published the largest single-centre cohort study so far with even higher survival rates of 69.5% (2 fetuses) and 91.8% (1 foetus)<sup>34</sup>.

However, FLOVA is still associated with high complication rates<sup>34</sup>. In particular iPPROM is a common but dangerous complication. iPPROM almost always results in preterm delivery, which is associated with higher mortality and neurological impairment rates. Stirnemann et al. even argues that with the improvements in surgical techniques and perinatal outcomes, postoperative complications have shifted to non-lethal obstetric complications, such as iPPROM<sup>35</sup>. In a large retrospective research of more than 1000 cases, Stirnemann et al. found the iPPROM rate to be increasing from 15% in 2000 to 40% in 2016. This increase in iPPROM occurred along an overall improvement of survival (42% to 66% for 2 fetuses).



# Chapter 3

---

## *Introducing Fetoscopic Laser Oclussion of Vascular Anastomoses in the Radboudumc*

3.1	Introduction . . . . .	16
3.2	Infrastructure and Materials . . . . .	17
3.3	Procedures and Protocols . . . . .	20
3.4	Monitoring and Reporting . . . . .	23
3.5	Training and Schooling . . . . .	27
3.6	Discussion . . . . .	30
3.7	Conclusion . . . . .	31

---

## 3.1 Introduction

Since the introduction of foetal therapy, there is a constantly increase in the number of IFTC. This could (temporally) lead to less favourable outcomes due to the 'learning curve effect'<sup>4,5</sup>. Thereby, there are enormous differences in practice between foetal therapy surgeons, which makes it difficult to compare the quality of work among different centres<sup>36</sup>. There is a need for a more standardized approach. This could benefit the outcomes of foetal therapy as also the quality of research and even the quality assurance. Currently, there is a lack of uniform worldwide evidence-based guidelines, which results in experience based practice.<sup>36,37</sup>

The lack of uniform protocols and guidelines makes it difficult, for hospitals with the ambition to start an IFTC, to implement foetal therapy. The best guideline for the implementation of foetal therapy in the Radboudumc is a national quality norm for IFTC published by Vandebussche et al.<sup>1</sup> in 2016. The quality norm on invasive foetal therapy defines requirements for a Dutch IFTC as a whole, for the procedure, the surgeons, the counselling, the long-term care and the way to report and monitor all proceedings. The quality norm was used to ensure a successful implementation of foetal therapy in the Radboudumc.

The Radboudumc aims at an introduction of foetal therapy in early 2018, starting with the implementation of the FLOVA procedure. This report documents all the steps and decisions that were take in the implementation process. Hopefully, this documentation could be a guideline for other hospitals with the ambition to start an IFTC.

---

## 3.2 Infrastructure and Materials

The first area of the quality norm concerns all the infrastructure and materials important for the FLOVA procedure. The infrastructure is of major importance for the management of TTTS and the success rate of the FLOVA procedure. The quality norm states that patients should be consulted and treated within 24 hours. This requires a dedicated and specialized foetal therapy team, special facilities and a large number of foetal therapy equipment. Since, the Radboudumc wants to reduce the chance of complications of the FLOVA procedure, much care was put in finding new and innovative equipment that could prevent these complications.

### 3.2.1 Foetal Therapy Team

A foetal therapy team should include a variety of disciplines, among which maternal-foetal medicine specialists, geneticists, paediatric surgical specialists, obstetric anaesthesiologists, neonatologists, ultrasonographers specialized in the diagnosis of foetal anomalies, and dedicated foetal therapy nurses.<sup>38</sup> In the Radboudumc all these specialisms are included, as can be seen in table 3.1. The foetal therapy team consists of two experienced gynaecologists in foetal therapy and two gynaecologists in training for the specialization of foetal surgery. In addition, the team consists of two technical physicians who perform research towards foetal therapy. Furthermore, these specialists provide ongoing support on all the technical aspects of foetal therapy.

**Table 3.1** Overview of all foetal therapy specialists with their function within the foetal therapy team.

<b>Foetal therapy specialist</b>	<b>Function</b>
Foetal surgeon	Performing foetal therapy and surgery, counselling and regular patient meetings.
Obstetric anaesthesiologist	Maternal management during obstetric or foetal interventions.
Neonatologist	Prenatal consultation, peri-partum and post-delivery care to fetuses and follow-up on treated patients.
Foetal therapy nurse	Care coordination and resource for patients.
Ultrasonographer	Performing advanced foetal ultrasound examinations during regular check-ups and the FLOVA procedure.
Psychosocial worker	Coordination of social services, patient advocacy and perinatal loss support.
Technical physician	Research towards foetal therapy, ongoing support on all the technical aspects of foetal therapy.

---

### 3.2.2 Facilities

The IFTC will be located in the Amalia children's hospital of the Radboudumc. This hospital incorporates both the prenatal phase at the prenatal diagnosis and obstetrics department as well as the perinatal phase at the neonatology department. The prenatal diagnosis department will facilitate the regular ultrasound examinations and the outpatient clinic visits. The obstetric department will facilitate the care around the birth and delivery. The neonatology department, with 17 NICU beds, will facilitate in postnatal care if necessary.

Most (70%) IFTC perform there operations in the general operating room<sup>33</sup>. Only a small percentage (30%) of the centres performs there operations in a outpatient operating room or a dedicated foetal surgery room. In the Radboudumc, the procedures will be performed in the general operating room.

### 3.2.3 Materials

A standard set of fetoscopic equipment usually consists of a fetoscope, a fetoscopic sheath, a cannula and a laser fibre. In addition, FLOVA requires a camera system and a laser device.<sup>39</sup> The diameter of the fetoscopic instruments varies between 1-4 mm and is different among IFTC<sup>36</sup>. Most IFTC use 10 Fr. instruments for posterior placenta's and 12 Fr. instruments for anterior located placenta's. In general, a operating sheath is used in combination with a large scope and a laser fibre. A larger fetoscope size results in a larger field of view and a better orientation during the procedure. However, larger instrument diameters also result in more complications.<sup>6,40,41</sup> In 2012 Beck et al. proposed to use smaller instruments, if possible, to overcome iatrogenic damage<sup>6</sup>.

As a result, in the Radboudumc, we decided to split the procedure in a orientation and a coagulation phase. During the orientation phase, solely a fetoscope is used while during the coagulation phase a smaller fetoscope in combination with a operating sheath and a laser fibre is used. Hereby, it is possible to use instruments with a maximum diameter of 8 Fr. for the treatment of a posterior located placenta and 9 Fr. for an anterior located placenta. The laser source that will be used in the Radboudumc is a 980 $\mu$ m Diode laser with a maximum wattage of 100 watt, as used in most IFTC centres<sup>36,39</sup>.

**Rod lens Fetoscope** During the orientation phase of the procedure Rod lens scopes will be used to make an overview of the placenta. This scope provides high resolution and wide angle views needed for the placenta reconstruction software. For the posterior located placenta's a Hopkins 2.0 mm 0°fetoscope will be used.

---

For the anterior located placenta's a 2.9 mm Rod lens scope will be used to make an overview of the placenta. This scope has a forward oblique view of 30° in order to provide a better view on the anterior placenta.

**Fiber Fetoscope** During the laser phase of the procedure the Rod lens scope will be replaced by an operating sheath combined with a 1.3 mm fibre scope and a 550  $\mu\text{m}$  laser fibre. For posterior located placenta's a straight 8 Fr. operating sheath is used. For anterior located placenta's two curved 9 Fr. operating sheaths are available: a 30° or a 60° degrees variant. The location of the anterior placenta in respect to the entry point will determine the choice of sheath.

**Uretero-renoscope** Even with the use of a 60° operating sheath, parts of the vascular equator of an anterior located placenta could be inaccessible. Since, the optimal energy impact is obtained at an angle of 90° in respect to the vessels, multiple techniques have been proposed in order to provide better access to the placenta<sup>42</sup>. In the early stages of foetal therapy, Deprest et al. tried to get a better access to anterior located placenta's by performing an laparotomy<sup>43</sup>. Middeldorp et al. tried to access the placenta posteriorly via laparoscopy<sup>44</sup>. Today, most of the foetal therapy centres use a special fetoscope with a deflecting mechanism for the laser fibre. However, these scopes have a diameter of at least 12 Fr.

To our knowledge we are the first IFTC to use an uretero-renoscope (URS) to visualize inaccessible locations on an anterior located placenta. This steerable scope, with a small working channel for the laser fibre, can be used to access and laser the unapproachable locations of the placenta. The URS will be used in combination with a 365  $\mu\text{m}$  diameter laser fibre, to allow for more movement of the scope. More important, the URS is compatible with the 9 Fr. access used for an anterior located placenta.



**Figure 3.1** The flex X2S uretero-renoscope (URS) of Karl Storz. The URS can be manually controlled and steered. The small working channel is used to insert the laser fibre.<sup>45</sup>

---

## 3.3 Procedures and Protocols

The procedures and protocols are a second important topic that needs to be addressed before introducing the FLOVA operation. The quality norm on invasive foetal therapy states that an IFTC should have clear disease specific protocols. These protocols should contain information about all aspects of the FLOVA process meaning the pre-operative, peri-operative and post-operative phase. Therefore, the FLOVA protocols concern for example the procedure, the counselling and the long term care. The quality norm defines requirements for all those subjects. Much care and effort was put in designing innovative and complications preventing protocols.

### 3.3.1 Protocols

An overview of the complete FLOVA protocol can be found in figure 3.2. The FLOVA protocol describes the process from the diagnosis of TTTS until the treatment of TTTS with FLOVA.

#### Pre-operative

When a patient with a possible TTTS is detected in the Radboudumc or referred to from another hospital, an appointment is made on the prenatal diagnosis department (<12 h.). At the outpatient clinic a diagnostic advanced ultrasound examination is performed by a specialized ultrasonographer. If a TTTS is diagnosed based on the Quintero classification system and a FLOVA procedure is indicated, the examination is followed by a counselling interview with the foetal surgeon and a psychosocial worker. The counselling follows the specific requirements of the quality norm and the content of the counselling was agreed on beforehand by the complete IFTC team. Patients also receive the information on paper and are given sufficient time to make their decision. After informed consent is received, the patient is scheduled for the FLOVA procedure. The operation is planned at least within 24 hours after the arrival of the patient.

#### Peri-operative

The FLOVA procedure is started and ended with a short briefing with the complete foetal therapy team. Thereby, a coordinator will be appointed to guide and lead the procedure. All communication between the personnel is performed in closed-

---

loop to prevent errors. Like most foetal therapy centres we decided to perform the FLOVA procedure under local anaesthesia and intravenous sedation<sup>36</sup>. The location of the entry point is determined by the foetal surgeon and the ultrasonographer. The actual FLOVA procedure is divided into two parts: the orientation and the coagulation phase. During the orientation phase the complete vascular equator is visualized and marked between the anastomosis. A drawn map of the placenta is made on a whiteboard by the assisting foetal surgeon. After the orientation phase of the procedure, all anastomoses are coagulated according to the SQLCPV technique. Consequently, the SOLOMON procedure is performed. The procedure is ended by amniotransfusion.

## **Post-operative**

After the procedure, the patient is admitted to the obstetrics department for about 24 hours. Within 24 hours after the operation an advanced ultrasound examination is performed to assess the condition of the fetuses and the success of the procedure. Consequently, the patient is discharged from hospital. The advanced ultrasound examination is repeated after 1 week, thereafter biweekly until birth.

### **3.3.2 Prospective Risk Assessment, Mock-up and Training**

The procedure specific protocols were designed and composed with the help of the complete IFTC team. Multiple meetings were arranged to discuss the methods and materials for the procedure and to make a draft version of the protocols. Literature was consulted to search for new and innovative ways to enhance the FLOVA operation and to reduce the risks for complications.

Weekly training sessions were organized in order to test the protocols. After every training session the protocols were evaluated and revised if necessary. A prospective risk assessment with the complete IFTC team (see table 3.1) was performed in order to evaluate the draft versions of the protocols and to remove possible errors and ambiguities.

At last, the final protocols were tested during a mock-up of the FLOVA operation, with special attention to crew resource management. The complete IFTC team simulated the operation in a realistic environment. The mock-up took place in the OR with sterile equipment. A debriefing was organized to evaluate the performance and to revise the protocols. Thereafter, the protocols were uploaded to Q-portal in order to allow the complete IFTC team to access. The protocols are continually revised when necessary.

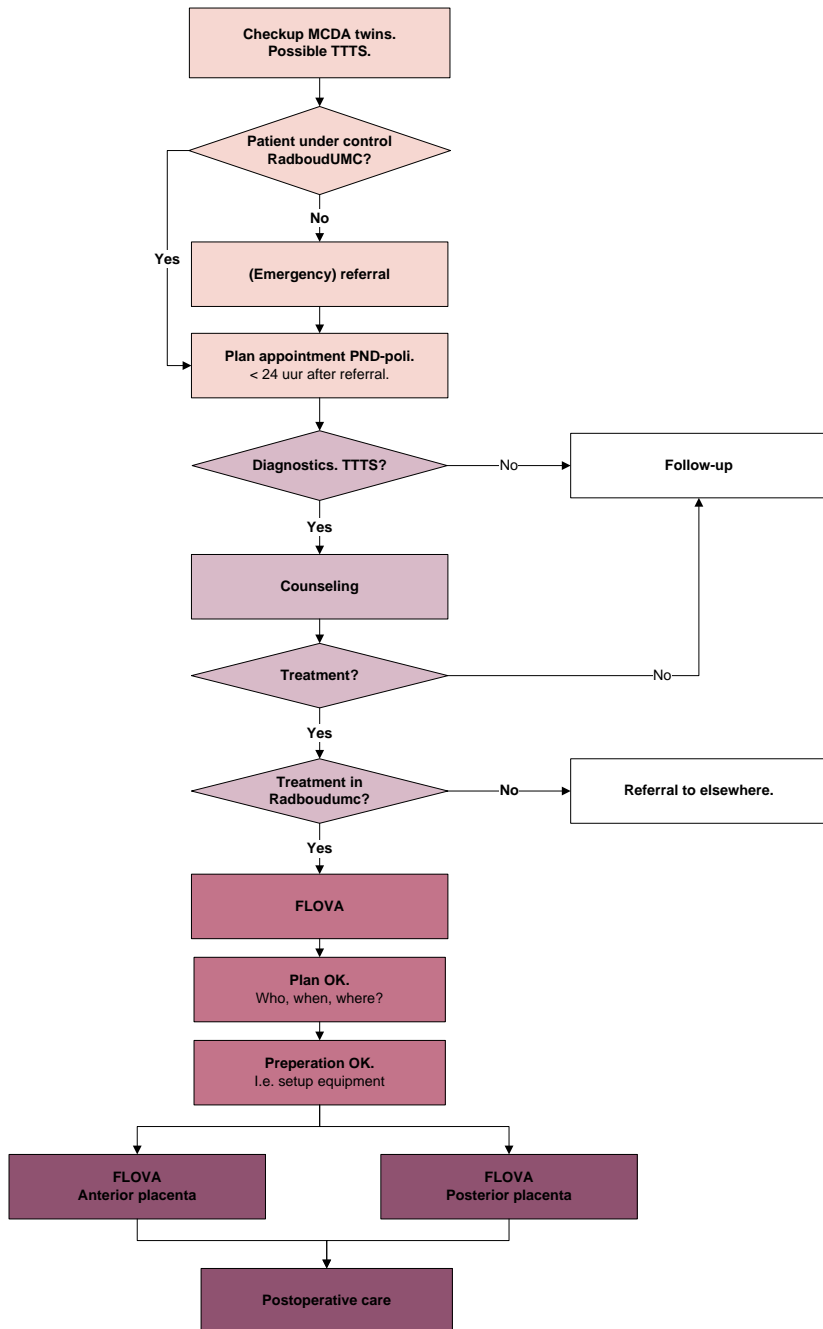


**Figure 3.2 Overview of the FLOVA protocol.** The protocol describes the care path for TTTS patients, from arriving in the hospital to the postoperative care.

---

## 3.4 Monitoring and Reporting

The fourth area includes the monitoring and reporting of the foetal therapy proceedings. The quality norm on invasive foetal therapy states that regular monitoring and reporting on the performance and results of the FLOVA procedure are needed. This is needed for quality control, transparency and to improve counselling for future proceedings. An extensive protocol was written on what and how to monitor the different parameters important for the FLOVA procedure. The protocol was sent for ethical approval to the Central Committee on Human Research (CCMO).

The collected patient data will be used to monitor and assess the quality of care in case of the FLOVA procedure. With the data it is possible to monitor the surgery from the moment it is implemented in the Radboudumc. This creates the opportunity of determining the learning curves of the surgeons regarding this operation. In addition the collected data will be used for the development of the 3D reconstruction software for artificial field of view expansion of fetoscopic videos during foetal surgery.

### 3.4.1 Monitoring

For the quality assurance and the research towards the 3D placenta reconstruction software multiple parameters will be monitored. The monitoring parameters were chosen based on literature, the quality norm and the opinion of the foetal therapy team. Both pre-operative and peri-operative as well as post-operative parameters are included.

#### **Procedural Parameters**

Table 3.2 shows all the procedural related parameters that will be prospectively collected of patients treated with FLOVA. These parameters will be used to determine the surgical learning curves. Furthermore, we would like to use these parameters to create a tool that can be used to calculate the estimated survival rate for an individual patient. This tool would allow us to compare the pre-operative estimated survival rates with the postoperative results, which could give insight in the performance of IFTC.

**Table 3.2** Overview of all the monitoring/research parameters. From every patient these parameters are prospectively assessed and stored in Castor EDC.

<b>Pre-operative</b>	
	<b>Quintero stage</b> <b>Gestational age</b> <b>Cervical length</b> <b>Placenta localization</b> <b>Ultrasound parameters:</b> - MVP
<b>Per-operative</b>	
	<b>Materials:</b> - Optics - Introducers - Laser fibre - URS <b>Anastomoses:</b> - Number - Types - Locations - Order of coagulation <b>Surgery times:</b> - Introduction - Orientation - Coagulation - Exit <b>Laser:</b> - Time - Maximum wattage - Total amount of energy <b>Complications:</b> - Foetal (i.e. IUFD) - Maternal (i.e. blood loss)
<b>Post-operative</b>	
	<b>Outcome:</b> - Foetal - Maternal <b>Complications:</b> - Foetal (i.e. iPPROM, IUFD or rTTTS) - Maternal (i.e. inflammation)

---

## Fetoscopic Videos

During the surgery, fetoscopic videos will be acquired. This fetoscopic videos will be used to develop and test software which will be able to create a 3D reconstruction of the placenta. Ex-vivo testing gave promising results leading us towards in-vivo testing. The videos are used to test and optimize the software before it will be implemented into the clinic. The feasibility of using the software in the clinic is also assessed.

## Placenta Examination

After giving birth and delivering the placenta, the placenta of all patients will be collected, stored and examined, according to the protocol of Jelin et al<sup>46</sup>. All placentas are washed and amnions are removed. Thereafter, the umbilical veins and arteries are cannulated and injected with a solution of water and paint. Realistic colours are used, to resemble the in-vivo situation. At last, umbilical cord clamps are used to occlude the vessels. Photos of the placenta will be made and stored in the research database. In addition, the dye-injected placenta will be inspected and potential findings will be noted.

The dye-injected placenta will be used in order to evaluate the results of the FLOVA surgery with the surgeons. Furthermore, the photographed dye-injected placentas will be used to visually compare the created 3D reconstruction with the real-life situation.



**Figure 3.3** Monochorionic placenta dye-injected with realistic colours. The umbilical cords are indicated with clamps.

---

## **Follow-up**

All children that were born after they were treated with FLOVA, will undergo follow-up on their neurological development. At 2 years the children will undergo standardized neurological testing at the specialized follow-up poli of the neonatology department. At the age of 6, children and parents will be asked to fill in the standardized ages and stages questionnaire.

### **3.4.2 Data Storage**

All the patient data will be stored in Castor EDC. The patient number corresponding with the record numbers from Castor EDC are stored in an encrypted file on the Radboudumc server, which can only be accessed by the researchers of this study. The Digital Research Environment (DRE) of Radboudumc will be used to store the fetoscopic videos and the placenta photos.

### **3.4.3 Evaluation and Reporting**

In consultation with the expert team and based on the requirements of the quality norm evaluation moments were agreed. The Radboudumc will report, on a yearly basis, on the total number of sessions. Every two years more details on the performances of the IFTC will be published. The reports will be available for all (referring) specialists, paediatricians, boards of hospitals, insurance companies, and also to the public.

---

## 3.5 Training and Schooling

The third area important for the introduction of an IFTC, is the required training and schooling for foetal therapy. With the need of a more standardized approach, much attention is given to training, schooling and quality control. The quality norm on invasive foetal therapy states that an IFTC should be in the possession of a setting and the instruments for ex-vivo training. The norm also gives some requirements for the foetal surgeons. The Radboudumc has employed one highly experienced and one moderately experienced foetal therapy surgeon. Furthermore, two gynaecologists aim at becoming a foetal therapy surgeon as well. Training sessions are needed to ensure a level of expertise for all four surgeons.

### 3.5.1 Training

In the Radboudumc, a setting for ex-vivo training was developed in order to enhance the performance of all the IFTC team members. A realistic training environment and setup were created. Both were based on the hospital specific protocols and related literature. The layout of the training sessions was based on the needs and preferences of the foetal therapy surgeons. Literature on medical training was consulted, in order to provide didactic education.

In-vitro training is organized on a weekly basis. Training takes place at the outpatient operating room of the gynaecology and obstetrics department. A separate training set with all the foetal therapy equipment was created and is stored in a mobile cabinet at the department. Both the foetal surgeons as well as the nurses and technical physicians attend the training sessions.

#### Setup

Multiple setups with different purposes were created for the training sessions. When constant feedback on the performance of the surgeon is requested a transparent box is used to resemble the uterus. This allows the participants to follow the operations of the surgeon. For a more realistic situation a black box is used. In both cases the boxes are filled with water and an entrance port is created using tape. The realistic setup for the training sessions is made with either a dye-injected placenta or a 3D placenta phantom.



**Figure 3.4 Setup for the foetal therapy training.** (a) foetal therapy equipment, (b) live video footage of the fetoscopic procedure, (c) diode laser, (d) white-board for manual placenta mapping, (e) camera and light supply, (f) surgery phantom: plastic container, filled with water and a 3D placenta model.

Dye-injected monochorionic placenta's are used to train on posterior located placenta's. The use of real placenta's enables the possibility to also train the coagulation phase of the procedure. A 3D placenta model was designed in order to train on anterior located placenta's. One dye-injected monochorionic placenta was selected and taken to the 3D lab of the hospital where 3D photos were taken (figure 3.5). The 3D photos were converted into a 3D model and 3D printed in plastic. At last, the model was painted by hand. A special coating ensures the placenta to be waterproof.

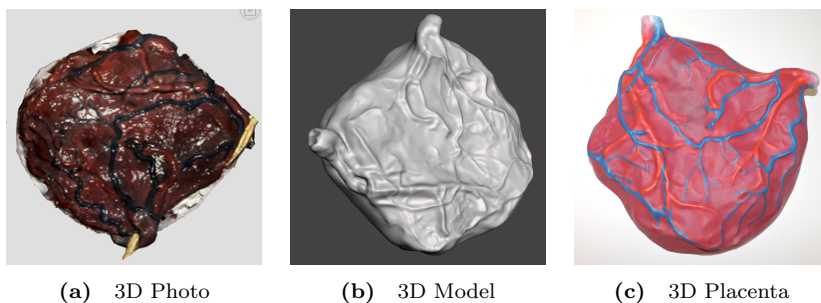


**Figure 3.5 Overview of the production steps of the 3D placenta phantom.** (a) 3D Photo of a dye-injected monochorionic placenta, (b) 3D model made out of the 3D photo of the monochorionic placenta, (c) 3D printed and painted model of the monochorionic placenta.

---

## Topics

In 2015 Peeters et al. published a study towards the most important steps during a FLOVA procedure<sup>37</sup>. 18 Steps were defined and the order of importance was determined. This showed that making sure that all the vascular anastomoses that cross the vascular equator are coagulated, is most important. However, these steps were identified by operator experience and not by evidence-based research on the outcome that is related to the taken steps. Yet, the 18 steps are used for the training sessions.

During the training sessions parts of the procedure as well as the complete procedure are trained. The surgeons can train on the visualization of the placenta as well as on coagulating the placenta vessels with the diode laser. Furthermore, much time was spend on learning to control and use the URS. At last, time was spend on the communication in closed-loop and team work between the foetal therapy team members.

### 3.5.2 Schooling

With all the adaptations that were made to the standard FLOVA procedure, namely the use of smaller diameter instruments, the use of an URS and in the near future the use of placenta reconstruction software, the Radboudumc aims at improving the FLOVA procedure in case of safety and efficiency. We would like to share this information and knowledge by starting an international schooling program on foetal therapy. In this way we hope to contribute to the foetal therapy care in both new and existing IFTC. A few IFTC, for example the Kings College Hospital in London and the University Hospitals in KU Leuven Belgium, offer nonaccredited foetal therapy fellowships already<sup>36,38</sup>. However, we aim to develop a more standardized and formalized accredited training program in foetal therapy.

---

## 3.6 Discussion

After years of preparation, the Radboudumc finally started an IFTC in January 2018. With the introduction of foetal therapy, the Radboudumc houses the second IFTC of the Netherlands, providing care for the eastern part of the country. Until this moment one patient was successfully treated for TTTS in the Radboudumc. In this report we documented the complete implementation process.

The strength of this project lies in the precision at which the introduction of the foetal therapy in the Radboudumc was performed. Much effort was put in the various steps of the introduction, from the purchase of the materials, the design of the protocols till the regular training. The prospective risk analyses and mock-up contributed to the well prepared protocols and a better collaboration between the foetal therapy team members. Thereby, the IFTC meets all the requirements of the quality norm on invasive foetal therapy.

We are aware that some of our innovative choices and methods are new and thereby not proven effective in literature. The use of two fetoscopes, one for the orientation and one for the coagulation, enables us to use smaller diameter instruments. However, this requires an additional step during the FLOVA procedure as the fetoscopes need to be changed. Research is needed to determine if or methods lead to more favourable results for the FLOVA procedure. Hereby, we will also take into account the use of the 3D placenta reconstruction software. Our hypothesis is that this new method could result in less complications, shorter operation times and better foetal outcomes.

The following years will be important for the future of the IFTC. The quality norm on invasive foetal therapy states that a starting period of 3 years should be enough to reach the minimum number of 20 procedures per year. This number should be enough to reach and maintain an acceptable level of performance for each of the surgeons. The upcoming months much effort will be put in acquiring a higher number of referred patients by publishing our work and innovative ideas. Furthermore, we are working on the introduction of FETO in the Radboudumc. At this moment, the Tracheal Occlusion To Accelerate Lung growth (TOTAL) trial is performed in the University Hospital of Leuven. Until the end of the trial all patients with CHD are referred to this hospital. After the results of the TOTAL trial are published we would like to introduce the FETO procedure in the Radboudumc as well. The preparations for this introduction has already started with the purchase of all the materials and a regular training session.

---

## 3.7 Conclusion

In January 2018, the Radboudumc started the second IFTC of the Netherlands, by implementing the FLOVA procedure. The introduction process followed the available literature and the national quality norm on invasive foetal therapy. Adaptations to the standard and most frequently used protocols were made to overcome the complications and problems of the FLOVA procedure. Thereby, research towards an innovative 3D placenta reconstruction method is performed. The following years will be important for the future of the IFTC. Together with the FLOVA, the introduction of the FETO should provide enough procedures to reach the minimum number of 20 procedures per year within 3 years.



# Chapter 4

---

## *3D Reconstruction of Fetoscopic Videos for Artificial Field of View Expansion during Foetal Surgery*

4.1	Introduction . . . . .	34
4.2	3D FLOVA-SLAM . . . . .	36
4.3	Image Acquisition . . . . .	38
4.4	Camera Calibration . . . . .	42
4.5	Feature Extraction . . . . .	50
4.6	3D Reconstruction . . . . .	59
4.7	Texture Reconstruction . . . . .	66
4.8	Discussion . . . . .	70
4.9	Conclusion . . . . .	72

---

## 4.1 Introduction

During the FLOVA operation all vascular anastomoses that cause the TTTS syndrome are sought-after and coagulated. The success of this operation relies on the condition that all the anastomoses will be identified. Therefore, the surgeon scans the placenta surface with a small fetoscope until all vascular anastomoses between the two twins are visualized. The locations and types of these anastomoses are memorized by the surgeon. Thereafter, the vessels are coagulated in a specific order so that the unbalanced foeto-foetal blood transfusion can be restored. This method leads to difficulties in the orientation and navigation for the surgeon. The limited field of view of the fetoscope together with a lack of proper landmarks on the placenta and poor visibility conditions complicate the FLOVA procedure. Increasing the fetoscope diameter would improve these conditions and possibly solve the issues. However, a larger fetoscope diameter will also lead to more iPPROMs, recurrent TTTS en TAPS<sup>6,40,41</sup>. A complete overview of the placenta could support the surgeon during the operation with the orientation while identifying all anastomoses and the navigation while coagulating the vessels in a certain order.

### 4.1.1 Placenta Mapping

A placenta map can be generated in various different ways. Most methods use the fetoscopic data that is acquired during the FLOVA procedure and use 2D image mosaicking to stitch the video frames<sup>47,48,49</sup>. In addition, some research is focused on using MRI or ultrasound to make a placenta overview. Werner et al. tried to describe the virtual 3D view of the placenta using MRI images<sup>50</sup>. Multiple other researchers tried to create a placental map by combining ultrasound images with fetoscopic images, both acquired during the procedure<sup>51,52,53,54</sup>. Other research focused on the use of laser speckle contrast imaging or electromagnetic (EM) and visual tracking, for placental mapping<sup>55,56</sup>.

None of these methods is already implemented in daily clinical practice, mainly due to the poor placenta reconstructions. Thereby, most of these methods are not usable in real-time and therefore they can not be used during the FLOVA procedure. In addition, all of these methods require additional hardware and are therefore subjected to operational constraints, which hinders the acceptance of the use of these methods for the FLOVA procedure.

---

### 4.1.2 Research Objective

The research objective of this study is to develop a novel method to create a real-time 3D overview of the placenta during the FLOVA operation. We investigated self-contained software methods that use only the fetoscopic output. In this work we present the complete framework for the 3D FLOVA-SLAM reconstruction method.

---

## 4.2 3D FLOVA-SLAM

For the placenta reconstruction method, self-contained software that only uses fetoscopic data is preferred. This can be achieved by using feature detection and matching, in which correspondences between image frames are used to calculate the geometric transformation of the camera and to reconstruct the placenta surface. Multiple researchers already conducted research into this topic. Most research is performed towards frequently used feature extraction methods like, SIFT, SURF and FAST<sup>47,48,49,57</sup>.

Most research in the area of placenta mapping is focused on image stitching or image mosaicking. With these methods the extracted features are used to calculate the transformation between two consecutive video frames, and to stitch the frames together. Daga et al. and Fransson et al. already showed promising mapping results using this method under laboratory conditions<sup>48,49</sup>. However, own research towards 2D image stitching in a more realistic ex-vivo setting, showed moderate to poor results in terms of the final placenta map. A major disadvantage of 2D image stitching methods is the accumulating error over time. Furthermore, these methods do not allow for 3D reconstruction and can not be executed in real-time.

Structure from Motion (SfM) and Simultaneously Localization and Mapping (SLAM) are both methods that can be used to reconstruct 3D environments. The use of 3D Reconstruction instead of 2D mapping reduces the positional error, since the fetoscope moves from a fixed point. Both SfM and SLAM methods use feature detection and feature matching in order to produce a 3D point cloud of an environment. The differences between both methods are illustrated in table 4.1. To our knowledge, there is no previous research into SfM or SLAM for the application of placental mapping. Since, the fetoscopic video frames are acquired in a ordered sequence, SLAM is the most logical candidate for a 3D placenta reconstruction method. Thereby, using SLAM allows for real-time rendering due to the relative low computational costs.

**Table 4.1** Comparison between Structure from Motion (SfM) and Simultaneously Localization and Mapping (SLAM).

SfM	SLAM
Unordered sequence of images.	Ordered sequence of images.
Large scale	Small scale
Acquisition with different camera's possible.	Acquisition with only one camera possible.
High computational burden.	Low computational burden.
Bundle adjustment and pose-graph optimization on all images.	Bundle adjustment and pose-graph optimization only on selected images.
Real-time rendering not possible.	Real-time rendering possible.

---

In conclusion, our approach uses feature extraction and visual-SLAM to calculate the camera positions over time and to reconstruct the placenta surface in 3D. Real-time texturing is added in order to provide the surgeon with an accurate representation of the placenta.

### 4.2.1 Framework

Figure 4.1 shows the complete framework for the 3D placenta reconstruction method: 3D FLOVA-SLAM. The framework comprises five primary steps, see below. These steps are described in more detail in section 4.3-4.7.

1. **Image acquisition.** During FLOVA procedures, videos of the placenta are acquired using a small fetoscope. These videos are used for the real-time 3D reconstruction.
2. **Camera calibration.** At the start of the operation a set of calibration images is acquired with a custom made sterilisable calibration plate. These images are used to calculate the camera parameters and calibrate the camera.
3. **Feature extraction.** All acquired video frames are processed with a feature extraction method.
4. **3D visual-SLAM.** The extracted features are plotted in a 3D point cloud and used to calculate the camera poses. The map is constantly updated by bundle adjustment and loop closing.
5. **Texture reconstruction.** A dense surface of the placenta is created on the 3D point cloud by mesh-generation. This mesh is formed by triangulation. Thereafter, the textured keyframes are mapped on this surface using the computed camera poses.

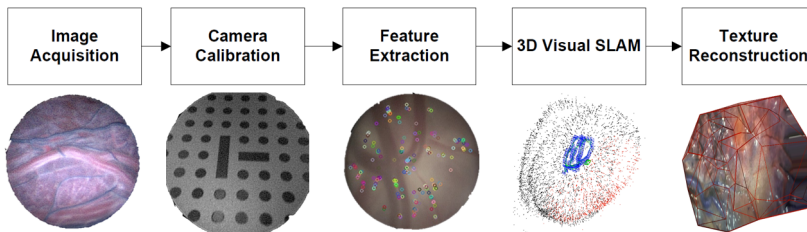


Figure 4.1 Overview of the five-step 3D FLOVA-SLAM reconstruction algorithm.

---

## 4.3 Image Acquisition

### 4.3.1 Introduction

The first step for the 3D reconstruction software is the acquisition of the fetoscopic images. During the FLOVA operation the actions of the surgeon are visualized by the fetoscope. These images provide the surgeon with the necessary information of the procedure. In addition, we can use these images directly for the 3D FLOVA-SLAM. However, this brings extra requirements for the hardware and software of the image acquisition. In order to acquire high quality and useful fetoscopic footage the image acquisition method must meet some important requirements, which are shown below. We searched for a combination of hardware and software that can meet these requirements.

- **Quality:** the quality of the fetoscopic videos, in terms of resolution, illumination and field of view, should be sufficient for the consecutive steps of the 3D FLOVA-SLAM framework.
- **Easy:** the acquisition of the fetoscopic videos should be easy and straight forward, so it would not limit the surgeon in his actions during the procedure.
- **Fast:** the acquisition of the fetoscopic videos should be fast enough to allow real-time rendering. A frame rate of at least 10 fps is preferred, to allow sudden movements of the surgeon.

### 4.3.2 Rod Lens Hopkins Fetoscope

In the Radboudumc the FLOVA procedure is conducted with a 2.0 mm or 2.9 mm rod lens Hopkins fetoscope during the orientation phase and a 1.3 mm fibre scope during the coagulation phase. In 2017, research towards the use of the 1.3 mm fibre scope or the 2.0 mm rod lens scope, in combination with our preliminary placenta reconstruction method showed promising results for the rod lens Hopkins fetoscopes<sup>58</sup>. The rod lens fetoscopes acquire images with high resolution and wide angles views that are needed for the 3D reconstruction software. With the Hopkins 2.0 mm fetoscope the largest average number of features and feature matches was found. Subsequently, this led to the best results regarding the reconstructed placenta image. The 2.9 mm rod lens Hopkins fetoscope potentially performs even better than the 2.0 mm scope, since the field of view of that scope is larger. For that reason, we decided to use the rod lens fetoscopes, see figure 4.2, for the image acquisition of the 3D FLOVA-SLAM software.



**Figure 4.2 Fetoscope.** Rod lens Hopkins 2.0 mm 0°fetoscope of Karl Storz<sup>59</sup>.

### 4.3.3 Karl Storz Camera

The fetoscope is used in combination with a Karl Storz Image 1 Hub HD. camera, with a resolution of 1920 \* 1080 pixels. This resolution was chosen, since feature detectors tend to have better accuracy at higher resolution images<sup>60</sup>. The data is acquired with a frame rate of 30 fps. A high frame rate was chosen in order to increase the probability of finding feature matches between consecutive frames<sup>49</sup>. A Karl Storz Cold Light Fountain Power Led 175 light source is used to illuminate the image scene. To enable a fast and easy acquisition, the camera is directly connected via DVI to an external laptop. The video footage is directly loaded into our software in Matlab or C++. In figure 4.3 an example of an acquired video frame can be seen.

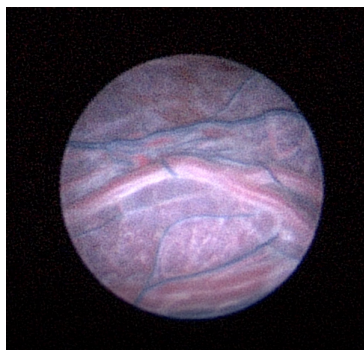


**Figure 4.3 Fetoscopic video frame.** Fetoscopic video frame of a dye-injected placenta acquired with the rod lens Hopkins 2.0 mm 0°fetoscope.

---

### 4.3.4 Discussion

The image acquisition for the 3D FLOVA-SLAM software will be performed with Hopkins rod lens fetoscopes. These scopes acquire images with high resolution and wide angles views that are needed for the 3D reconstruction software. In addition, the Hopkins fetoscopes are already used during the FLOVA procedure and therefore no different instruments or actions are needed.

Most articles on fetoscopic placenta mapping do not give details on the fetoscope that is used during their experiments<sup>48,49,57</sup>. Only Reeffer et al. documented the use of a 3.8 mm 12° endoscope, considerably larger than our Hopkins scopes<sup>61</sup>. With the change of PPROM being quadratically correlated to the diameter of the fetoscope, the use of scopes larger than our Hopkins fetoscopes seems undesirable<sup>41</sup>. Most researchers, acquire their fetoscopic data with a resolution of 1920\*1080, as in our method. However, in their methods the image frames are cropped to allow real-time rendering.<sup>48,49</sup> Optimization of the image resolution with regards to computational efficiency and feature extraction accuracy is needed.

The quality of the rod lens Hopkins fetoscopic videos meets our predetermined requirements for the image acquisition and is sufficient for the 3D FLOVA-SLAM software. The Hopkins fetoscopes acquire high resolution images. The connection between the camera and the computer is optimized by using a direct DVI connection, and enables us to subtract full HD (1080p) video frames. Only the use of a 4K UHD camera or a larger Hopkins fetoscope could improve the resolution of the images further.

The acquisition of the fetoscopic video frames is easy and straight forward since the videos are directly loaded into the 3D reconstruction software. This enables handling the image acquisition by the surgeon, without obstructing the clinical process. The image acquisition does not take extra time our effort and thereby shows high potential to be used during the procedure. To further our research we plan to design an clear interface that the surgeon can use for the control of the 3D reconstruction software.

Moreover, future research will focus on the optimization of the 3D reconstruction software in order to make it robust and independently of the type of fetoscope that is used. At this moment, the Hopkins fetoscopes are used for the orientation phase of the procedure, during the coagulation phase a smaller fibre scope or URS is used. This potentially leads to a longer operation time since a change of scopes is required. Furthermore, the current method makes live tracking during the coagulation phase impossible as another scope is used. Further improvements will lead to more generally usable software which enables the use of only one fetoscope during the procedure, live-tracking during the complete procedure and easier use for other IFTC.

---

### 4.3.5 Conclusion

At this moment, small rod lens Hopkins fetoscopes are used for the image acquisition during the FLOVA procedure. A high quality and fast connection between the camera and the computer allows real-time rendering of the fetoscopic videos. Further work will focus on creating a more robust 3D reconstruction method that is also compatible with other fetoscopes.

---

## 4.4 Camera Calibration

### 4.4.1 Introduction

Pinhole cameras, like an endoscope or fetoscope can have significant distortions. Especially cameras with a fish-eye lens, as the rod lens fetoscope show high positive radial distortions. These camera distortions can be corrected by performing a geometric camera calibration. For the 3D FLOVA-SLAM software a highly accurate representation of the real world is needed. An accurate camera calibration is vital for both the feature detection and the 3D reconstruction of the placenta surface.<sup>62</sup>

In order to perform accurate and easy calibrations, an automatic and robust calibration method has to be developed. To achieve this the calibration method must meet some important requirements, which are shown below.

- **Accurate:** reliable and accurate camera calibration results are important for the consecutive steps of our software. Much attention must be paid to optimize the calibration method and to ensure a small reprojection error.
- **Robust:** it is important that the camera calibration algorithm can handle imperfect conditions. It should be able to process images with vignetting artefacts due to the light source of the camera, specular reflections and perspective distortions.
- **Automatic:** it should be possible to handle the calibration system automatically. This in order to prevent errors, to ensure reproducibility and to fasten the procedure. This means that after the image acquisition, the image selection, the feature extraction and the calculation of the intrinsic and extrinsic calibration parameters must be automated. Ideally the calibration could be performed by the surgeon.
- **Sterile:** the camera calibration will be performed just before the FLOVA operation. Therefore, the calibration must be performed in a sterile environment. A sterilisable calibration plate and setup are essential.
- **Fast:** since the camera calibration will be part of the operation it is important to ensure a fast calibration method. In total the camera calibration should not exceed two minutes.

---

## 4.4.2 Calibration Pattern

For the camera calibration numerous calibration patterns are available. The most frequently used calibration patterns are chessboard patterns, see figure 4.4a<sup>63</sup>. These patterns have the advantage that they are easy to construct and their natural interest points make it easy to extract features. Furthermore, multiple calibration patterns are build out of dots, see figure 4.4b and 4.4c<sup>64</sup>. These circular patterns can be potentially more accurate but are also more complex to use in terms of mathematics.<sup>65</sup> For our software we first considered three possible patterns which can be seen below.

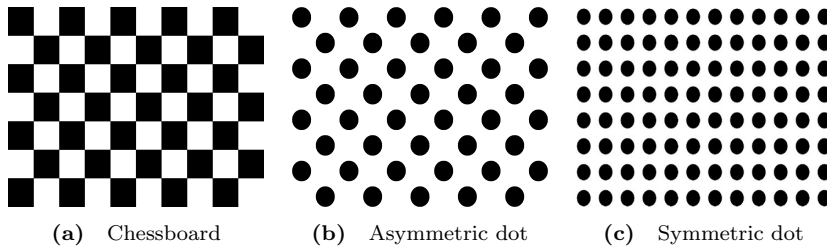


**Figure 4.4** Camera calibration patterns. (a) Chessboard pattern, (b) asymmetric dot pattern, symmetric dot pattern.<sup>66</sup>

Of all three patterns the use of the chessboard pattern was preferred because of the many open source algorithms that are available for processing the chessboard images. The circular patterns were preferred in case of accuracy important for the consecutive steps of our software. However, all three patterns appeared to be unuseful for our purpose since it is not possible to cover the entire endoscopic area with a rectangular image. A pattern which can cover the entire image area ensures a complete undistortion of the images including the highly distorted edges. Zooming in and taking only a part of the pattern on the image, ensures a full coverages but is not possible due to the symmetric nature of the patterns. For the calibration it is important to know the orientation of the calibration plate. In that case a pattern with an identifiable object in the middle is required.

Therefore, we chose to use a special grid illustrated in figure 4.5. This calibration pattern was designed by Reeff et al. and already proved to be successful for the calibration of endoscopic cameras.<sup>47</sup> The calibration pattern consists of a grid of black dots on a light gray background. These dots have a diameter of 1 mm and are 1 mm apart. In the middle of the calibration pattern two rectangles are situated which are needed to encounter the orientation of the symmetric pattern. The smaller bar defines the x-axis, the larger bar the y-axis. These bars need to be visible in every calibration image.

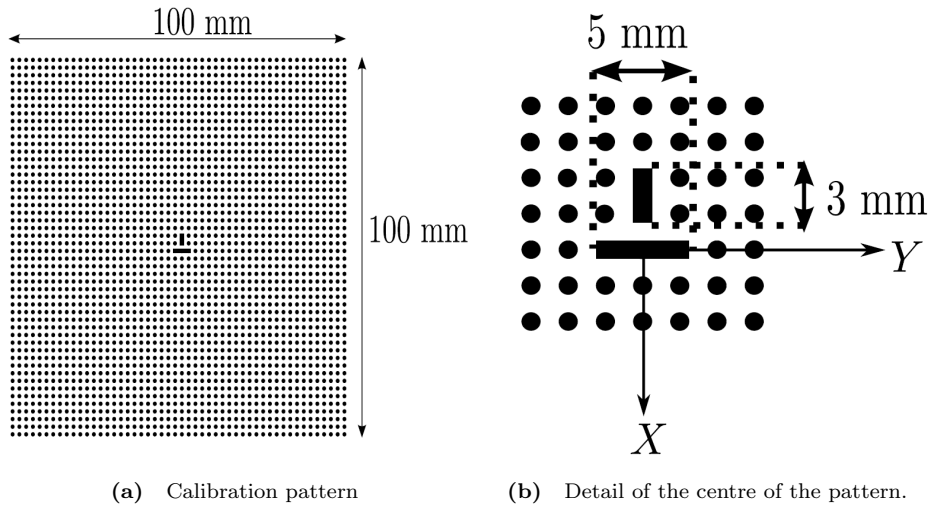


**Figure 4.5 Special calibration pattern.** (a) Calibration pattern, (b) detail of the two bars in the centre of the calibration pattern.<sup>47</sup>

The Medex Instruments company produced a CE-registered calibration plate with the special calibration pattern (figure 4.6). The calibration plate is made from mat stainless steel which makes it sterilisable for use in the OR and non-reflective. The size of the plate is 11 x 11 cm<sup>2</sup> and it is 2 mm thick preventing it from bending.

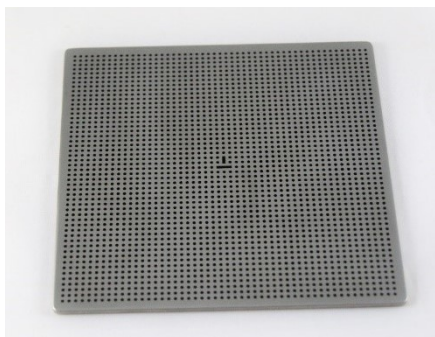
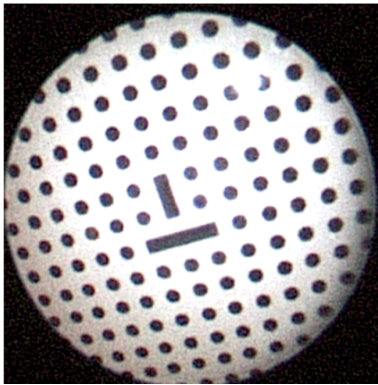


**Figure 4.6 Metal sterilisable calibration plate.** The plate is specially designed for the 3D FLOVA-SLAM software. The calibration plate will be used to calibrate the fetoscopic camera during the FLOVA procedure.

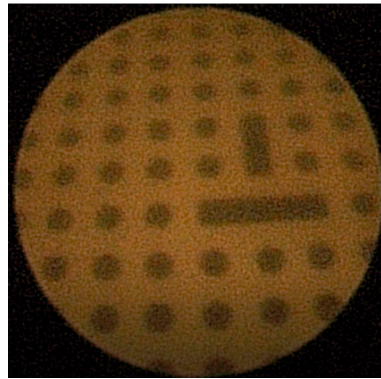
---

### 4.4.3 Calibration Setup

Since the FLOVA operations are performed in the amniotic cavity, it is presumed that the camera calibration must be performed in amniotic fluid as well<sup>47,49</sup>. The intrinsic parameters of a camera change when it is placed in different media. In figure 4.7 two calibration images are shown, one taken into clear water, one taken in amniotic fluid. The amniotic fluid can be collected before the surgery by amnion drainage.



(a) Water



(b) Amniotic fluid

**Figure 4.7 Calibration images taken in two different media.** (a) Water, (b) amniotic fluid. Note the difference in colour and visibility.

During the image acquisition both the calibration plate and the tip of the fetoscope must be placed in the amniotic fluid in a sterile container, see figure 4.8 For the image acquisition we tested two possibilities: acquiring a video or acquiring multiple images. During the testing phase we concluded that taking videos increases the potential error, due to motion artefacts and the difficulty of keeping the identifiable objects in the image. Consequently, we decided to capture 15-20 images of the calibration pattern from different viewpoints for the camera calibration. The camera must be held at a distance of approximately 2-3 cm of the calibration pattern, the same distance as from the placenta during the FLOVA operation. The complete calibration protocol can be found in appendix A.



(a) Calibration plate inside metal container. (b) Overview of the calibration setup.

**Figure 4.8 Overview of the camera calibration setup.** (a) The sterilised calibration plate is placed in a sterile container filled with demineralized water. (b) Calibration images are taken with the rod lens Hopkins 2.0 mm 0° fetoscope on a distance of about 2-3 cm.

#### 4.4.4 Calibration Method

The calibration images are used to calculate the camera parameters. The calibration method of Reeff et al. is used, to process all the images and to calculate the camera matrix (figure 4.9). The images are filtered and all objects in the calibration pattern are identified by feature extraction. These new image coordinates are matched with the known grid coordinates and a transformation matrix is computed. Thereafter, the calibration parameters are calculated using the Bouguets Camera Calibration Toolbox<sup>67</sup>. At this moment the algorithm is implemented in MATLAB. More details about the calibration method can be found in appendix B.

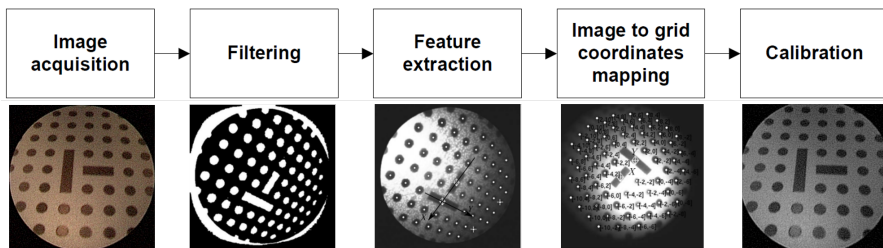


**Figure 4.9 Overview of the five-step camera calibration algorithm.**

---

### 4.4.5 Calibration Performance

The performance of the calibration tool was tested in an in-vitro environment. The test was performed in water due to a lack of amniotic fluid. Figure 4.10 shows an example of a distorted calibration image with the undistorted equivalent after the camera calibration. Table 4.2 shows the accuracy and elapsed time for the calibration in water. 19 Of 20 images were accepted and processed for the camera calibration. The mean back projection error is 0.56 pixels. The calibration process excluding the image acquisition takes about 24 seconds.

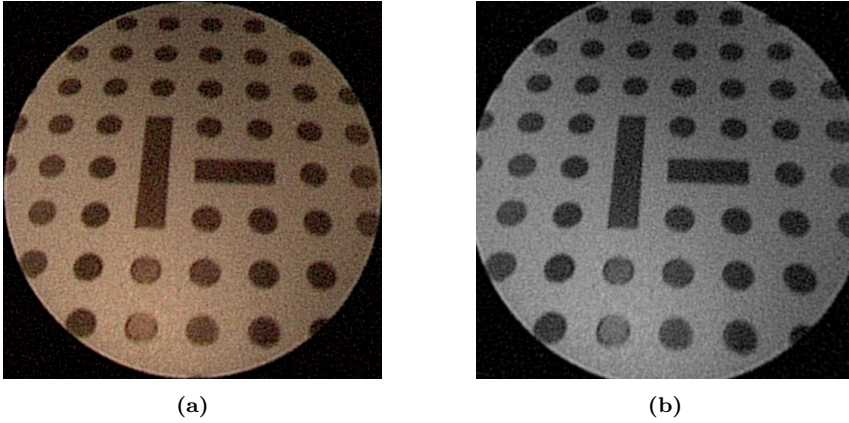


**Figure 4.10** Calibration images acquired with the rod lens Hopkins 2.0 mm 0°fetoscope. (a) Calibration image before the camera calibration and undistortion, (b) Calibration image after the camera calibration and undistortion. This left image shows the relatively small fish-eye distortion.

**Table 4.2** Results of one complete camera calibration. Twenty calibration images were acquired with the rod lens Hopkins 2.0 mm 0°fetoscope. All images were processed using the calibration software.

# Images Accepted	Error (pixels)	Time (sec)
19/20	0.578/0.547	24.06

---

## 4.4.6 Discussion

An adjusted version of the camera calibration method of Reeff et al. is used for the 3D FLOVA-SLAM software. Initial results showed good results regarding the undistorted images and a reasonable reprojection error of 0.56 pixels. When we compare our results with the results of Reeff et al. we find our error to be slightly higher, 0.56 in comparison with 0.4.<sup>47</sup> Another study towards this calibration method reported an average reprojection error of 0.25, however, these results were obtained with different endoscopes<sup>68</sup>.

The strength of our study lies in the extensive research that was done in order to find the best calibration method for this specific application. The camera calibration is extremely important for an accurate 3D reconstruction. However, a lot of articles on fetoscopic reconstruction do not take into account this important step<sup>49</sup>. Others, use the camera calibration method of Zhang et al., in combination with a chessboard pattern, implemented in the Matlab toolbox.<sup>53,63,69</sup> More research is needed to objectify the results of our calibration method with respect to other methods. Furthermore, we expect that the camera calibration application can be optimized even more, i.e. by improving the filtering or feature extraction.

Compared with our predetermined requirements our camera calibration application scores well on the accuracy and robustness. The combination of the metal calibration plate with our calibration setup and protocol results in images that are easy to process for our camera calibration method, since the acquired images show little to none specular reflections and have a high contrast. Furthermore, the metal calibration plate is suitable for sterilization and makes the camera calibration possible during the operation.

The calibration application works only partly automatically. Especially, the image acquisition part of the method requires manual control. To improve our method, a camera assisted image acquisition method is desired. During the image acquisition, the algorithm can provide feedback on the image quality by showing the feature extraction in real-time. This method ensures useful images for the camera calibration and thereby improves the accuracy of the calibration. Furthermore, it would simplify the method and make it more suitable to use for the surgeons.

Automating the application would also speed up the process. With a computation time of 24 sec on average and an acquisition time of a about 3-5 minutes the camera calibration method is really time-consuming. Since, the camera calibration is performed in amniotic fluid, every second of the calibration process counts. A longer operation time, increases the risk of complications like iPPROM. Since, amniotic fluid mostly consists of water (99%), taking water as an medium for the camera calibration could be considered. More research and testing is needed to exclude any relevant difference.

---

#### 4.4.7 Conclusion

A special camera calibration method has been developed that can be used to calculate the camera parameters of a fetoscope. The method already proved to be accurate and robust. Furthermore, the application is suitable for the use in a clinical setting. More research and testing is needed to optimize and fasten the application.

---

## 4.5 Feature Extraction

### 4.5.1 Introduction

In our method image features are used for the image mosaicking and mapping. These features, for example corners, edges or blobs can be extracted using a feature extraction method. There is large variety of feature extraction methods, with different working principles.<sup>70</sup>

In order to extract high quality features, an automatic and robust feature extraction method has to be developed. To achieve this, the feature extraction method must meet some important requirements, which are shown below.

- **Robust:** the feature extraction algorithm should be able to detect features independent of scale, rotation, artifacts and noise, to allow the surgeon to move freely over the placenta surface.
- **Accurate:** the feature extraction algorithm should accurately detect the image feature locations since these locations are used for the image mapping.
- **Quantity:** the feature detection method should be able to detect and match enough features, to allow the calculation of the camera movement.
- **Fast:** the feature detection method should work fast enough to allow real-time rendering. With a frame rate of 30 fps, this means a computation time of less than 0.033 sec per frame is required.

### 4.5.2 SIFT vs. ORB

For the 3D FLOVA-SLAM software two possible feature extraction methods were evaluated: Scale-Invariant Feature Transform (SIFT) and Oriented FAST and Rotated BRIEF (ORB). SIFT is one of the most widely used feature extractors and already showed promising results for placenta mapping applications.<sup>49,61,71</sup> Earlier research, of our institution, towards different feature detection methods for the placenta mapping application, showed also great potential for SIFT<sup>72</sup>. Groot Koerkamp et al. compared 7 feature detection methods (BRISK, FAST, Harris-Stephens, Minimum eigenvalue, MSER, SURF and SIFT) and 5 feature descriptor methods (BRISK, FREAK, SURF, Block and SIFT). The combination of the feature detection and the feature description method of SIFT turned out to be most successful.

---

Another feature extraction method with great potential for our application is Oriented FAST and Rotated BRIEF (ORB)<sup>73</sup>. ORB is a combination of the FAST keypoint detector and BRIEF descriptor. It was proved to be a fast and efficient alternative to SIFT. In addition, ORB features are used for the latest developed SLAM method, called ORB-SLAM.

SIFT and ORB were compared based on their ability to extract features in fetoscopic images. Thereafter, the feature extraction method with the greatest potential was used for building the 3D placenta reconstruction software.

## Materials

An in-vivo fetoscopic video of a placenta was used as a test object for the comparison between the feature extraction methods. This video was obtained using the 2.0 mm rod lens Hopkins fetoscope. The video was saved as \*.avi, with a frame rate of 30 fps and a size of 1920 \* 1080 pixels. The data processing was performed using PYTHON and OPEN CV.

Two sets of in-vivo fetoscopic image frames, low-textured and high-textured, were used to test the feature extraction methods, see figure 4.11. To maximize the results of the feature extraction, pre-processing of the fetoscopic images was performed. Blur enhancement was achieved using a Gaussian function, contrast limited adaptive histogram equalisation (CLAHE) was used to increase the contrast in the images. In figure 4.11c the fetoscopic video frame can be seen after pre-processing.

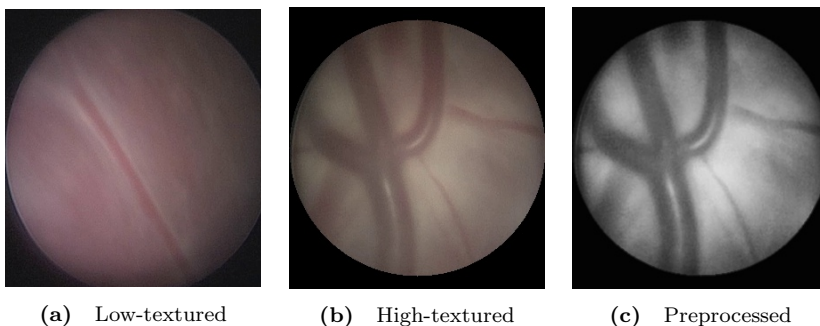


**Figure 4.11** Fetoscopic video frames acquired with the rod lens Hopkins 2.0 mm 0°fetoscope during a FLOVA procedure. (a) Low textured video frame with one small vessel, (b) high textured video frame with multiple large vessels, (c) preprocessed high textured video frame.

---

## Methods

SIFT and ORB were compared based on the pre-determined requirements. At first, the feature extraction methods were tested on their ability to find high quantities of features and feature matches. For each experiment the number of features found, the number of feature matches found, the matching rate and the computation time were determined. In this way, the methods were tested on their speed, accuracy and ability to find high quantities of features (matches). The brute-force (BF) matcher was used to calculate the feature matches. Random Sample Consensus (RANSAC) was used to determine the accuracy of the feature matches.

The robustness of the feature extraction methods was determined by testing the invariancy to scaling, rotating and an affine transformation. For these tests the image to be matched was adjusted. In case of rotation, a rotation of 45 degrees was applied on the second image. Furthermore, the image was scaled by a factor of 2, to test the scaling invariancy. At last, the image to be matched was sheared with a value of 0.5 to test the invariancy to shearing.

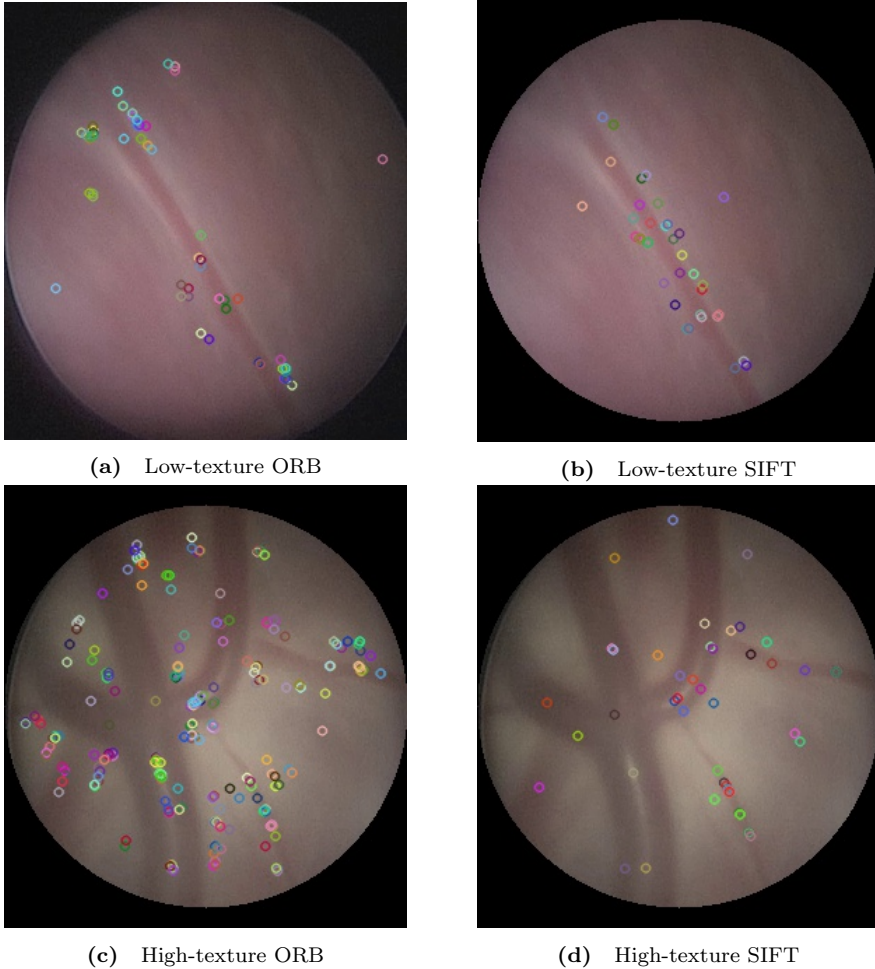
## Results

Table 4.3 shows the results of performing SIFT and ORB on the low-textured and high-textured image frames. For both image types, ORB outperforms SIFT on feature detection (figure 4.12). In the low-textured image a difference of 10 features is seen (31 SIFT vs. 41 ORB), in the high-textured image this difference is larger with more than 160 features in difference (219 SIFT vs. 52 ORB).

**Table 4.3 Results of SIFT and ORB feature detection and matching on two consecutive fetoscopic video frames.** Testing was done on a low-textured and a high-textured frame. The number of detected features and the computation time are denoted as an average number of the two consecutive video frames. The best method, SIFT or ORB, is displayed in green for every parameter.

<b>Low-textured</b>	<b>ORB</b>	<b>SIFT</b>
# Features (average)	41	31
Computation time (average)	0.003	0.074
# Feature matches	22	19
% Feature matches	42%	58%
<b>High-textured</b>		
# Features (average)	219	52
Computation time (average)	0.004	0.061
# Feature matches	106	34
% Feature matches	48%	65%

Figure 4.13 shows the result of feature matching with both ORB and SIFT. In both low-textured (19 SIFT vs. 22 ORB) and high-textured (34 SIFT vs. 106 ORB) images more feature matches are found with ORB. However, SIFT provides a better matching rate, in the low-textured images (58% SIFT vs. 32% ORB) and the high-textured images (65% SIFT vs. 48% ORB.). Furthermore, the computational speed of ORB is an order of magnitude faster than the computational speed of SIFT.



**Figure 4.12 Results of SIFT and ORB feature detection on the low-textured and high-textured fetoscopic video frames.** (a) ORB feature detection on the low-textured video frame, (b) SIFT feature detection on the low-textured video frame, (c) ORB feature detection on the high-textured video frame, (d) SIFT feature detection on the high-textured video frame.

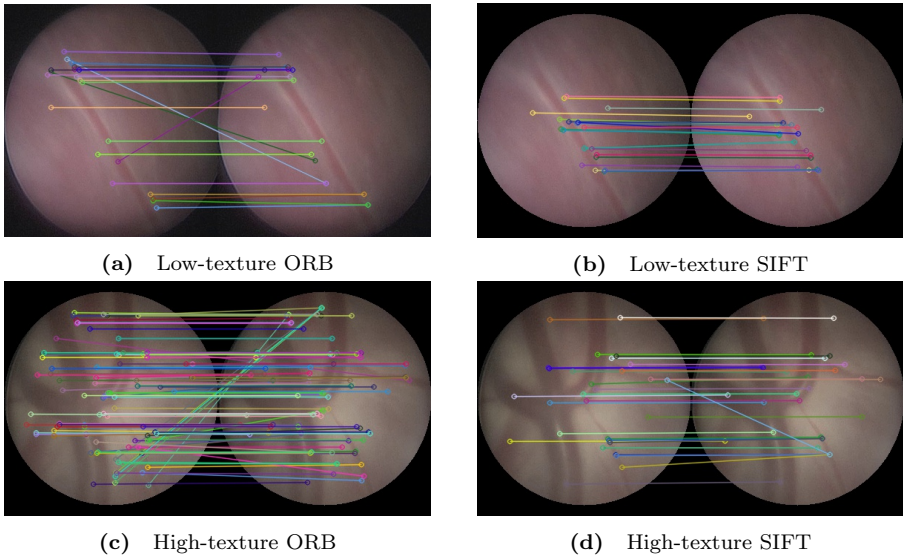


**Figure 4.13 Results of SIFT and ORB feature matching on two consecutive fetoscopic video frames.** Testing was done on a low-textured and a high-textured frame. (a) ORB feature matching on the low-textured video frame, (b) SIFT feature matching on the low-textured video frame, (c) ORB feature matching on the high-textured video frame, (d) SIFT feature matching on the high-textured video frame.

When ORB and SIFT are combined with RANSAC, all wrongly matched feature pairs are removed (figure 4.14). Table 4.4 shows the percentage of feature matches before and after applying RANSAC. As RANSAC is used to remove bad matches the percentage of feature matches decreases for both SIFT and ORB. The difference in decrease between ORB and SIFT is striking. The percentage of feature matches decreases with approximately 10% in ORB and around 30% in SIFT.

**Table 4.4** Results of SIFT and ORB feature matching in combination with RANSAC on two consecutive fetoscopic video frames. Testing was done on a low-textured and a high-textured frame. The best method, SIFT or ORB, is displayed in green for every parameter.

	ORB		SIFT	
<b>Low-textured</b>	Normal	RANSAC	Normal	RANSAC
# Feature matches	22	17	19	10
% Feature matches	42%	32%	58%	30%
<b>High-textured</b>				
# Feature matches	106	79	34	16
% Feature matches	48%	36%	65%	31%

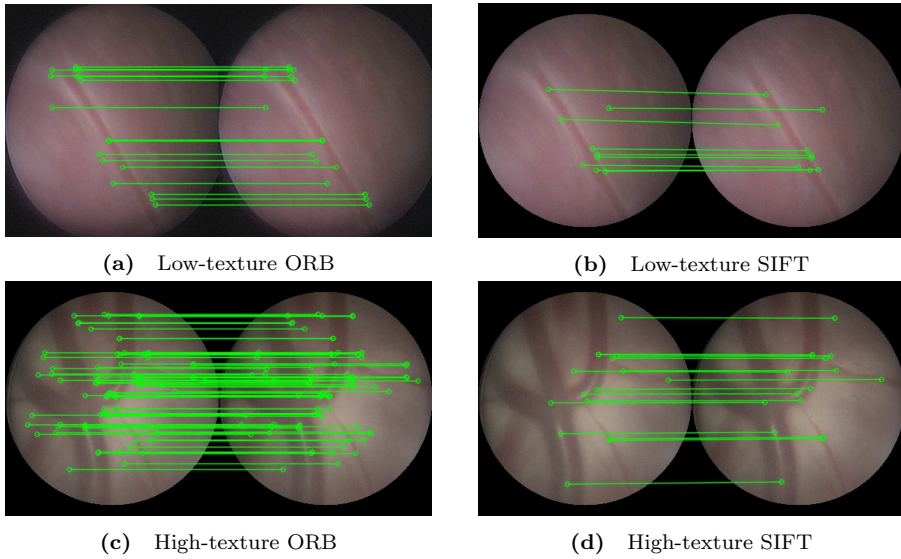


**Figure 4.14 Results of SIFT and ORB feature matching in combination with RANSAC on two consecutive fetoscopic video frames.** Testing was done on a low-textured and a high-textured frame. (a) ORB feature matching + RANSAC on the low-textured video frame, (b) SIFT feature matching + RANSAC on the low-textured video frame, (c) ORB feature matching + RANSAC on the high-textured video frame, (d) SIFT feature matching + RANSAC on the high-textured video frame.

The results of testing the invariancy to scaling, rotating and an affine transformation of ORB and SIFT can be seen in figure 4.15 and table 4.5. The results show that, in case of a scale, rotational or affine transformation, more feature matches are found with ORB. For both SIFT and ORB the rotational transformation has the largest negative influence on the results. The matching rates drop to 5% for ORB and 19% for SIFT. Figure 4.15 also shows that not all matches are correct even when RANSAC is applied.

**Table 4.5 Results of SIFT and ORB feature matching in combination with RANSAC on two consecutive fetoscopic video frames.** Three different transformations were applied on the second high-textured image: scaling, rotating and affine. The best method, SIFT or ORB, is displayed in green for every parameter.

	ORB			SIFT		
High-textured	Scale	Rotation	Affine	Scale	Rotation	Affine
# Feature matches	42	11	79	23	10	13
% Feature matches	19%	5%	36%	44%	19%	25%

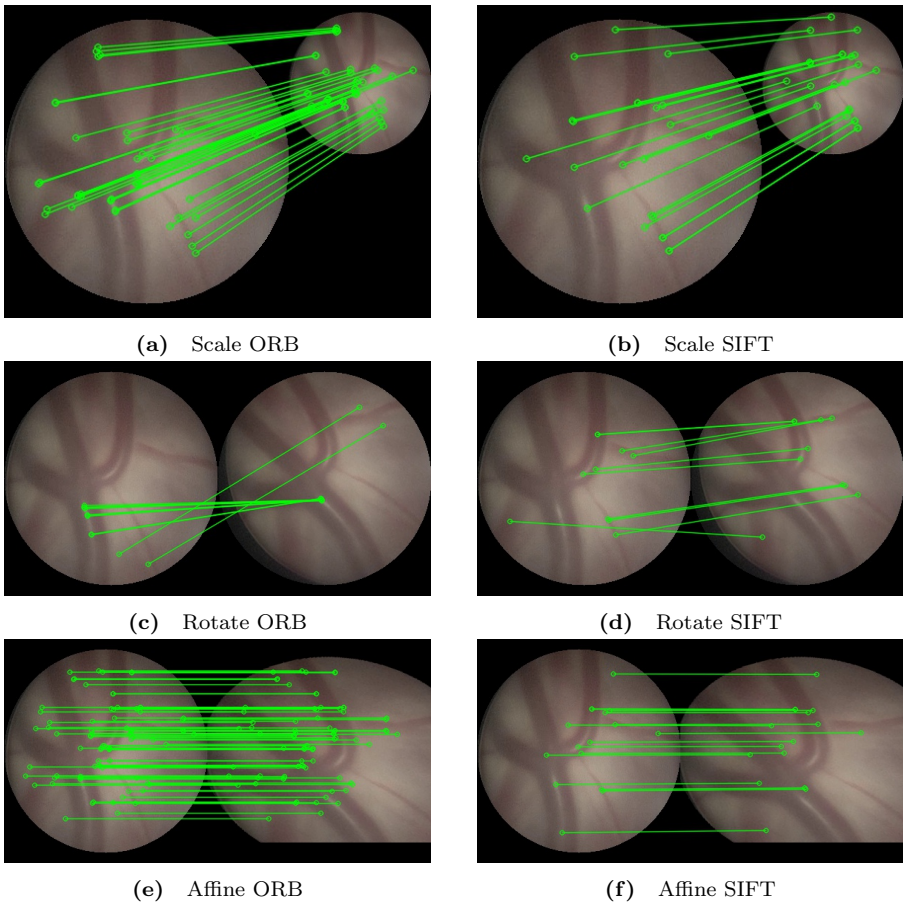


**Figure 4.15 Results of SIFT and ORB feature matching in combination with RANSAC on two consecutive distorted fetoscopic video frames.** Three different transformations were applied on the second high-textured image: scaling, rotating and affine. (a) ORB feature matching on the scale transformed high-textured video frame, (b) SIFT feature matching on the scale transformed high-textured video frame, (c) ORB feature matching on the rotational transformed high-textured video frame, (d) SIFT feature matching on the rotational transformed high-textured video frame (e) ORB feature matching on the affine transformed high-textured video frame, (f) SIFT feature matching on the affine transformed high-textured video frame.

---

### 4.5.3 Discussion

3D FLOVA-SLAM uses feature extraction to be able to calculate the camera movement and to reconstruct the placenta. Two potential feature extraction methods, SIFT and ORB, were compared on their ability to extract features on fetoscopic video frames. Experiments showed that more features and feature matches are found with ORB. Compared to ORB, SIFT results in a higher percentage of features that can be matched, also when a scaling or rotational transformation is applied. ORB results in more features and feature matches in case of an affine transformation. In addition, ORB outperforms SIFT on the computational speed.

Gaisser et al. also compared SIFT and ORB for the feature detection on placental images<sup>57,74</sup>. In contrast to our results, they found more features with SIFT compared to ORB. This could be explained by the difference in input data, in contrast to our in-vivo data, Gaisser et al. used ex-vivo phantom data. Thereby, they experimented with different media, i.e. yellow coloured water. Fransson et al. experimented with SIFT on in-vivo placental images, and found similar findings as in our research<sup>49</sup>. Karami et al. compared SIFT and ORB on their performance on distorted images<sup>75</sup>. They found a better performance for SIFT, in case of rotation or an affine transformation. ORB performed better than SIFT in case of a scaled image. This is not completely consistent with our results. However, these results need to be interpreted with caution since Karami et al. tested the performance on different image scenes.

By comparing the feature extraction methods in several different ways, we achieved to get a broad overview on their performances. In this way, we could evaluate the methods based on all our predetermined requirements. However, a limitation of our study is the large amount of parameters, i.e. for the preprocessing, that is used for both ORB and SIFT. The settings of these parameters have a large influence on the feature extraction, and therefore could bias the results. Although, parameters were chosen equal for both methods as much as possible.

Compared to the predetermined requirements we can conclude that both SIFT and ORB are moderately invariant to image transformations. For both methods the feature matching rate decreases if a transformation is applied. Both methods are most sensitive to rotation, with a decrease of 106 to 11 feature matches in ORB and 35 to 10 feature matches with SIFT. The performance of 3D FLOVA-SLAM on images with changing conditions, completely depends on the amount of SIFT or ORB feature matches that are needed for an accurate reconstruction. This numbers are currently unknown.

By looking at the results of applying RANSAC in combination with SIFT and ORB, we notice a large difference between SIFT and ORB. The percentage of feature matches decreases with approximately 10% in ORB and around 30% in

---

SIFT. This means that with SIFT more wrongly matched pairs are found in respect to ORB. The accuracy of ORB is better than that of SIFT when no RANSAC is applied. The large number of wrongly matched pairs probably also explains the differences between ORB and SIFT in terms of matching rate. However, it is not yet clear whether the accuracy of the ORB feature extraction is high enough for our 3D FLOVA-SLAM software. More research is needed to determine the actual accuracies of ORB and SIFT.

With ORB, higher quantities of features and feature matches are found in respect to SIFT. However, it is hard to determine if these numbers are high enough to allow an accurate calculation of the camera poses. Especially video frames of low-textured areas, with low rates of features and matches, could hamper a correct reconstruction. More research on the combination of feature detection and our 3D reconstruction method is needed to determine the quantities of features that are needed for an accurate end results. In terms of computational speed, ORB is more than an order of magnitude faster than SIFT, which is consistent with the literature<sup>73</sup>. With an average computation time of 0.0675, SIFT is thereby not fast enough for real-time rendering. Therefore, SIFT does not meet all the requirements that are important for our application. ORB does meet the requirement with an average computation time of 0.0035.

In conclusion, more features and more correct feature matches are found with ORB in respect to SIFT. Thereby, ORB outperforms SIFT in terms of speed and is suitable for real-time rendering. In addition, ORB is freely available in contrast to the patent protected SIFT. Furthermore, ORB is already implemented in one of the newest SLAM software packages. Ultimately, ORB was chosen for the feature extraction in the placenta mapping 3D FLOVA-SLAM software.

In order to combine the ORB feature detection and matching method with the 3D reconstruction method, small adjustments, i.e. a change of preprocessing, to the standard ORB application were made. More details about ORB as it is used for our 3D FLOVA-SLAM software can be found in appendix C.

#### 4.5.4 Conclusion

ORB outperforms SIFT on terms of feature detection, feature matching and computational speed. The SIFT method is thereby not suitable for real-time applications due to a high computational burden. In addition, SIFT is patent protected for commercial use, while ORB is freely available. Ultimately, ORB was chosen for the feature extraction in the 3D FLOVA-SLAM software.

---

## 4.6 3D Reconstruction

### 4.6.1 Introduction

The extracted ORB features can be used to estimate the camera motion and to reconstruct the 3D environment using SLAM. This reconstruction will be used for the orientation and navigation of the surgeon. Therefore, it is important that the 3D reconstruction method meets the following requirements:

- **Accurate:** the 3D reconstruction method should be accurate since it will be used to guide the surgeon during the FLOVA procedure. A Root Mean Square (RMS) error of less than 0.5 cm is preferred.
- **Robust:** the 3D reconstruction method should be robust to sudden movements. It should be able to relocate after tracking is lost.
- **Fast:** the 3D reconstruction method should work fast enough to allow real-time rendering, so that the surgeon can use the 3D reconstruction during the procedure. With a frame rate of 30 fps, this means a computation time of less than 0.033 sec per frame is required.

### 4.6.2 Visual-SLAM

#### Indirect vs. Direct SLAM

Visual-SLAM methods can be divided into direct and indirect methods. Direct methods use pixel intensities of the complete input images to calculate the camera position overtime. Indirect methods use feature extraction to locate the camera. Since, indirect visual-SLAM uses an abstract version of the input images, this method is potentially faster than the direct method. In addition, the indirect visual-SLAM method is more robust for changing imaging conditions than the direct method, since the direct method only works with pixel intensities. The direct method however, provides a more dense point cloud since it handles more image points.<sup>76,77</sup> A dense point cloud is useful when it is directly used without any post-processing steps. Since, the aim of the project is to texture the reconstructed 3D point cloud, a dense point cloud is not the biggest priority. Therefore, an indirect visual-SLAM method is preferred.

---

## Bundle Adjustment

Indirect visual-SLAM methods can be of two different type: filter-based or bundle adjustment-based. Mono-SLAM is a well-known filter-based visual-SLAM method that was developed in 2003<sup>78</sup>. Mono-SLAM uses an Extended Kalman Filter (EKF) in order to estimate the camera motion and to map the 3D structure simultaneously. This method has the problem of a high computational cost, when high number of features are extracted, and can therefore, not be used in real-time. The successor of MONO-SLAM is PTAM, a bundle adjustment-based method, in which the tracking and the mapping are executed in parallel which reduces the computational costs and allows for real-time rendering<sup>79</sup> (figure 4.16). Furthermore, this method uses bundle adjustment for the optimization step. The recently developed (2015) ORB-SLAM method also uses bundle adjustment for the optimization<sup>80,81</sup>. In addition, it uses pose-graph optimization which allows for loop closure detection. In ORB-SLAM, tracking, mapping and loop closure detection are executed in parallel.

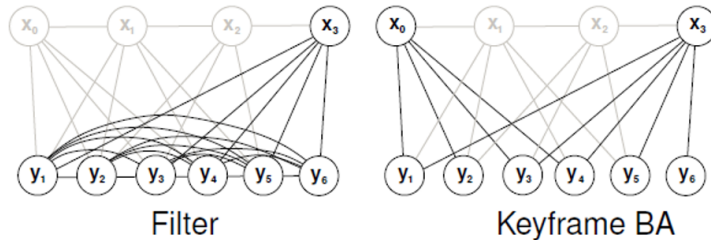


Figure 4.16 Filter based SLAM vs. Bundle adjustment based SLAM. <sup>82</sup>

Bundle adjustment based methods are more efficient compared to filter-based methods, even if the number of extracted features and keyframes is high<sup>83</sup>. Efficiency and speed are important requirements for our 3D placenta reconstruction method. Therefore, a bundle adjustment method seems to be most functional. Thereby, Strasdat et al. proved that BA-based methods are more accurate than filter-based methods<sup>82</sup>.

## Pose-graph Optimization

The continuously optimization in visual-SLAM is of great importance due to the accumulating error overtime. During the fetoscopic surgery the fetoscope will be moved over the placenta surface for about 20 minutes. There will be a lot of overlap in the acquired images. Next, to the bundle adjustment, pose-graph optimization can be used to reduce the error and to improve the generated map<sup>76</sup>. Pose-graph

optimization is used to link a current acquired image to a previously acquired image. The accumulated error can be set to the same value as of the first time an image frame was seen. Thereafter, the physical loop in the map can be closed.<sup>84</sup>

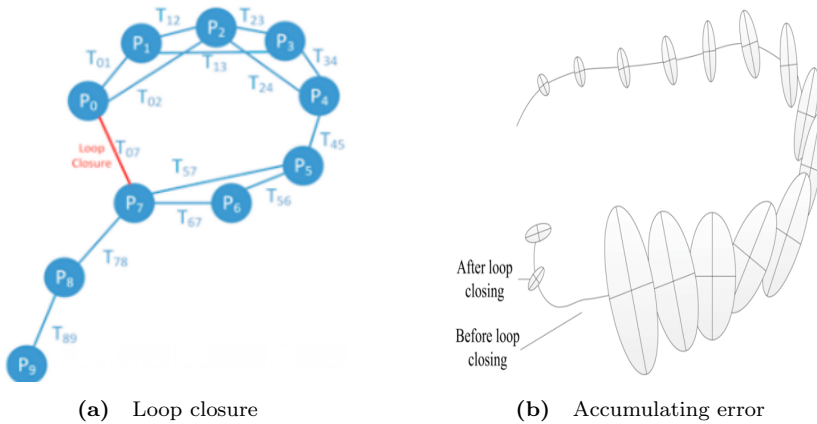


**Figure 4.17 Pose-graph optimization.** (a) the camera trajectory is estimated from relative pose measurements. The relative pose measurements are obtained from visual feature registration. Pose-graph optimization is used to identify and close loops. (b) loop closing results in an increase of the accumulated error.<sup>85</sup>

In contrast to MONO-SLAM or PTAM, ORB-SLAM contains a pose-graph optimization thread. This makes ORB-SLAM the most complete indirect monocular visual-SLAM system. Thereby, ORB-SLAM is also available as an open-source application. Furthermore, it already showed promising results in other medical applications. At last, ORB-SLAM uses ORB feature extraction, which turned out to be most successful for our application.

### 4.6.3 ORB-SLAM

ORB-SLAM turned out to be the most promising visual-SLAM method for our 3D placenta reconstruction software. Therefore, ORB-SLAM2 of Mur et al. was used for the 3D FLOVA-SLAM application<sup>81</sup>. ORB-SLAM2 is implemented in C++ and incorporates also ORB feature extraction. Figure 4.18 shows an example of the ORB-SLAM interface.

At this moment, ORB-SLAM is only completely functional with the use of a Logitech web-cam. Due to a problem with the camera calibration in combination with the fetoscope, ORB-SLAM is not functional on fetoscopic videos.

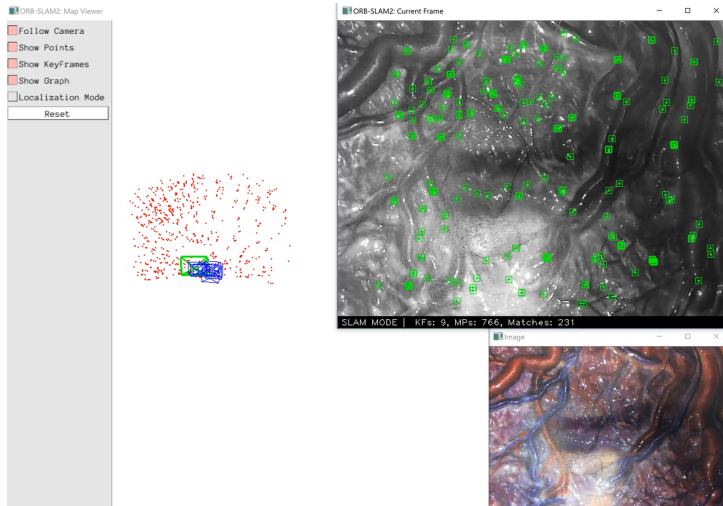


**Figure 4.18 ORB-SLAM interface.** On the left multiple visualization functions are displayed. In the middle the 3D point cloud (red), the camera trajectory (green) and the key frames (blue) are shown. On the lower right the original image is displayed, while on the upper right the feature detection in the current frame is shown.

The complete ORB-SLAM method exists of three main components which are executed in parallel: tracking, local mapping and loop detection (figure 4.19). The tracking thread takes care of the ORB feature extraction, the keyframe selection and the calculation of the camera movement.

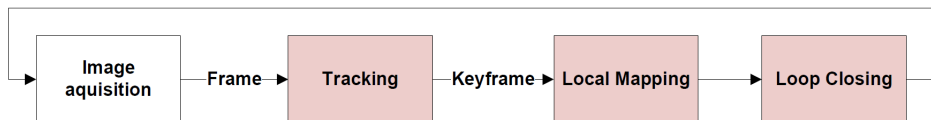


**Figure 4.19 Overview of the complete ORB-SLAM method.**The ORB-SLAM method exists of three main components which are executed in parallel: tracking, local mapping and loop detection.

The extracted features are used to calculate the movement of the camera. The local mapping thread handles the features by plotting them in a point cloud, as can be seen in figure 4.20. In addition, it plots the selected keyframes. The loop detection thread handles the just processed keyframes and tries to detect and close loops. Figure 4.21 shows an example of a loop closure. More details on the ORB-SLAM method can be found in appendix D.

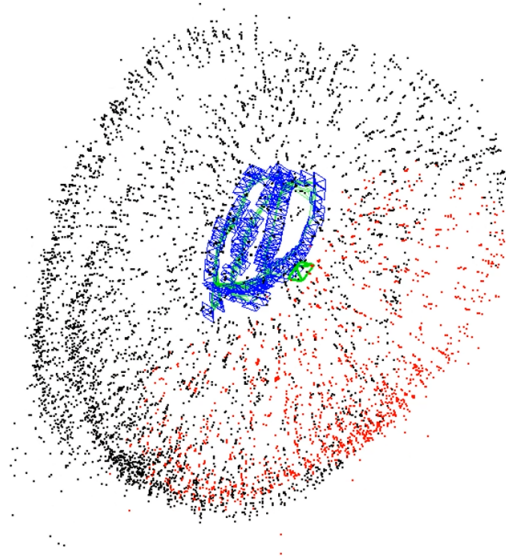


**Figure 4.20 3D Point cloud.** ORB-SLAM performed using a web-cam on a 2D placental image. The 3D point cloud (red/black) consists of all the extracted ORB features. The red dots are the features that are currently seen by the camera. The black features are found stable and therefore added to the database. Furthermore, the camera trajectory (green) and the key frames (blue) are displayed.

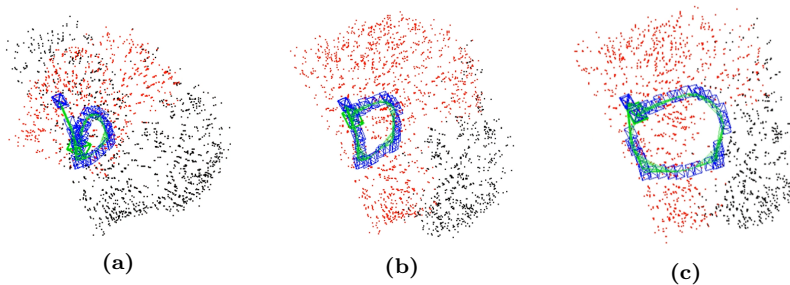


**Figure 4.21 Loop closure.** ORB-SLAM performed using a web-cam on a 2D placental image. Point cloud of three consecutive frames which display the loop closing function of ORB-SLAM. When the current keyframe is linked to a keyframe that was already seen before, ORB-SLAM tries to close the loop. (a) First image frame, before loop closing, (b) second image frame, right after loop closing, adjacent keyframes are corrected, (c) third image frame, after loop closing, all keyframes are corrected, duplicated map points are fused.

---

#### 4.6.4 Discussion

The 3D SLAM method for artificial field of view expansion during foetal surgery is based on ORB-SLAM. ORB-SLAM was implemented and adjusted to be able to process the fetoscopic images. The first results of testing the algorithm on placental images and phantoms show promising results. However, until this moment ORB is only completely functioning with the use of a web-cam. Due to a problem with the camera calibration in combination with the fetoscope, ORB-SLAM is not functional on fetoscopic videos.

3D FLOVA-SLAM is the first method to incorporate ORB-SLAM for fetoscopic placental mapping. Other fetoscopic mapping algorithms use 2D image stitching and do not incorporate a SLAM or SfM method to first calculate the movement of the camera, where after a 2D or 3D reconstruction is calculated. Also in other medical specialisms the use of ORB-SLAM is limited. Mahmoud et al. implemented ORB-SLAM to perform endoscope tracking and 3D reconstruction of abdominal endoscopic images<sup>86,87</sup>. He proved that the ORB-SLAM method is robust enough to be used for monocular endoscopic tracking and a dense 3D scene reconstruction. A second application of ORB-SLAM, was introduced by Qiu et al.<sup>88</sup>. Qiu et al. used ORB-SLAM to create a 3D reconstruction of the oral cavity. These applications and the 3D FLOVA-SLAM method have in common that they are aimed at low-textured medical images. More research into the use of ORB-SLAM on in-vivo video footage is needed to determine the performance in a more realistic situation.

ORB-SLAM is the most modern and advanced SLAM method at this moment<sup>76,89</sup>. Due to a combination of bundle adjustment, pose-graph optimization and loop closing ORB-SLAM outperforms earlier versions of SLAM, as for example MONO-SLAM. Earlier research of our own, was concentrated on using MONO-SLAM for the 3D FLOVA-SLAM application<sup>58</sup>. With the use of ORB-SLAM, the results of mapping the placental surface have extremely improved. Due to the accumulating error over time only 7 seconds of fetoscopic videos could be stitched using MONO-SLAM. Thereby, the application which incorporated MONO-SLAM could not be rendered in real-time. Due to the fast ORB feature extraction method and the parallel threads, ORB-SLAM can be rendered completely real-time. Thereby, ORB-SLAM meets the requirement of being fast enough.

The accuracy of the ORB-SLAM implementation is yet unknown. The accuracy of the 3D reconstruction is of great importance since it is used by the surgeon in his decision-making process. Coagulating the wrong vessels or passing the real anastomoses will have a negative effect on the foetal outcomes. In the nearby future, we aim to validate the accuracy of the 3D SLAM method, for example using EM or visual tracking. This method is used by multiple other researchers<sup>56</sup>.

---

The robustness of the 3D reconstruction method is the last important requirement. Different tests with the ORB-SLAM method showed the ability of ORB-SLAM to perform under constantly changing conditions. Only with fast and unexpected movements ORB-SLAM loses the track. However, due to the relocalization function, most of the times tracking can be resumed quickly. Only in areas of low-texture, where low amounts of features are detected, relocalization and initialization can be more difficult.

The following months more research towards ORB-SLAM in combination with the fetoscope will be performed. Thereafter, in-vivo testing will be performed to determine the abilities of ORB-SLAM on real fetoscopic videos.

#### **4.6.5 Conclusion**

The 3D SLAM method for artificial field of view expansion during foetal surgery is based on ORB-SLAM. Due to a combination of bundle adjustment, pose-graph optimization and loop closing ORB-SLAM outperforms other SLAM methods. Thereby, ORB-SLAM can be rendered completely real-time. The first results of testing the algorithm on placental images and phantoms show promising results. However, until this moment ORB-SLAM is only completely functional with the use of a web-cam. Future research will be aimed at validating the ORB-SLAM method and enabling the use of ORB-SLAM in combination with a fetoscope.

---

## 4.7 Texture Reconstruction

### 4.7.1 Introduction

The 3D reconstruction of the placenta gives the surgeon an idea about the dimensions of the placenta. However, it does not provide a detailed map of the placental vasculature needed for the orientation. In order to create such a map, it is needed to texture the 3D point cloud created with ORB-SLAM. For the texture reconstruction the following requirements are of interest.

- **Accurate:** the texture mapping should provide the surgeon with a detailed map of the placenta. The surgeon will use this map to determine the coagulation locations. Therefore, the map should accurately reflect the real situation.
- **Fast:** the texture mapping should work fast enough to allow real-time rendering.

### 4.7.2 Mesh-generation

Before the textured images can be mapped on the 3D point cloud, a mesh is generated. This mesh is needed to define a surface out of the sparse point cloud that is generated with ORB-SLAM. The mesh consists of multiple vertices (3D points) and faces (triangle of 3 vertices). In most texture reconstruction methods, the sparse point cloud is densified before the actual mesh is generated. For our application a dense reconstruction is thought unnecessary.

Multiple methods for mesh generation are available. For example the Poisson surface reconstruction and the Delaunay mesh generator<sup>85</sup>. Both methods already proved to be very accurate for medical applications<sup>90,91,92</sup>. For our method we chose the tetrahedral Delaunay meshing algorithm to generate our mesh surface, since it is easy to implement and to combine with ORB-SLAM.

At this moment, the mesh is generated on the 2D images. On every video frame the extracted features are used to create the mesh. Figure 4.22 shows an example of a created mesh on placental images.

..

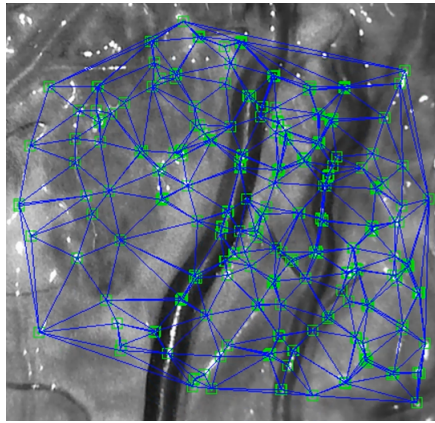


**Figure 4.22 2D Mesh-generation.** Delaunay 2D triangulation for mesh-generation. The detected image features are displayed in green, the mesh is shown in blue.

### 4.7.3 Texturing

For every vertex the corresponding 3D point is determined. Thereafter, the 2D generated meshes are transposed to the 3D space. Consequently, for every face, the corresponding texture is transposed on to the accompanying mesh in the 3D space. Figure 4.23 shows an example of a textured placenta reconstruction.

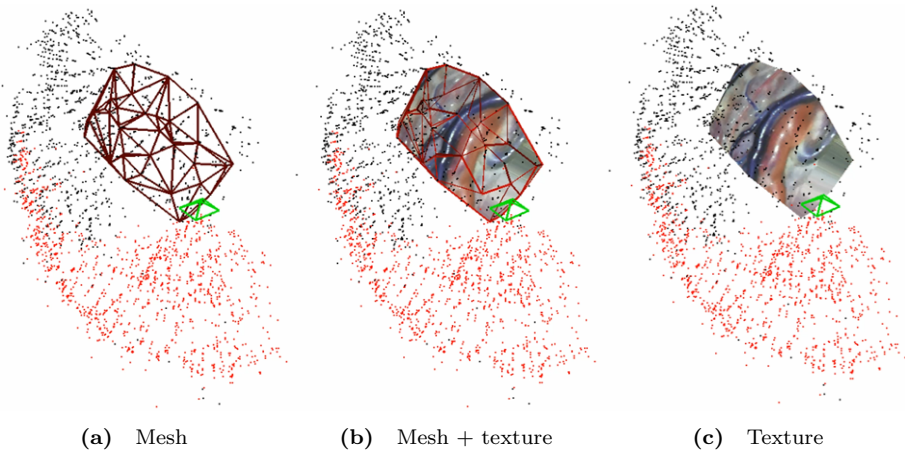


**Figure 4.23 Texture reconstruction.** ORB-SLAM performed using a web-cam on a 2D placental image. Texturing performed on one image frame. (a) The 2D generated mesh transposed to the 3D environment, (b) the 2D generated mesh transposed to the 3D environment, including the corresponding texture, (c) placenta texture in the 3D environment.

---

#### 4.7.4 Discussion

To complete the 3D placental reconstruction and to create a detailed overview map of the placenta, texture reconstruction is necessary. For the 3D FLOVA-SLAM software an initial texturing method and algorithm were developed. More research and experiments are needed to improve and finish the texture reconstruction method.

If our method succeeds, it would be the first method capable of real-time texturing in combination with SLAM. At this moment, texture reconstruction is only possible for offline methods, such as SfM. Also for medical applications, texture reconstruction is only performed after acquiring the data. Lurie et al. recently published an article on 3D textured reconstructions of the bladder made with SfM<sup>90</sup>. The complete pipeline and application of this method resembles the 3D FLOVA-SLAM method, except for the fact that it is not a real-time solution.

Lurie et al. used Poisson triangulation for the mesh-generation and found good results regarding the textured reconstruction. Foteinos et al. and Fedorov et al. both used the Delaunay triangulation for mesh-generation, as in the 3D FLOVA-SLAM software<sup>91,92</sup>. More research towards the different triangulation methods is needed to determine the best method for our solution.

In addition, further research will focus on implementing 3D triangulation and mesh generation. At this moment, multiple transformation between the 2D space and 3D space are needed in order to texture the 3D point cloud. In theory a direct texture reconstruction on the 3D point cloud will reduce the computational cost and speed up the process.

At this moment the texture reconstruction method is not accurate enough to be used by the surgeon in a clinical setting. More research into possible post-processing methods, such as blending, could enhance the results. The current texture reconstruction method allows for real-time rendering and therefore meets the stated requirement. After the completion of the texture reconstruction software, more experiments will be executed to determine the performance of the software.

---

### 4.7.5 Conclusion

The last step of the 3D FLOVA-SLAM is the texture reconstruction. At this moment an initial method, that incorporates mesh-generation and texturing, has been implemented. More research and experiments are needed to improve and finish the texture reconstruction software. Thereafter, 3D FLOVA-SLAM would be the first method to incorporate real-time texturing.

---

## 4.8 Discussion

The past year, a framework for an application that can artificially expand the field of view during the FLOVA procedure was developed. The application consists of five major steps: the image acquisition, the camera calibration, the feature extraction, the 3D reconstruction and the texture mapping. For all of the steps the best available method applicable to our problem was selected.

As far as we know this is the first application that can create a real-time 3D textured overview of the placenta using visual-SLAM. Most articles, focusing on placenta mapping, use 2D image mosaicking methods<sup>49</sup>. These methods have the problem of a large accumulating error over time, resulting in problems handling videos with a long duration. With the use of ORB-SLAM, the cumulative error is reduced by a constant loop closing thread. This enables processing fetoscopic video footage of the complete FLOVA procedure. Thereby, in many cases, ex-vivo results obtained by translating a fetoscope over a placenta look promising but in-vivo mapping using a fixed entry point remains difficult. By approaching the movement of the fetoscope as a 3D problem, we are able to create a complete 3D overview of the placenta even when the placenta is encountered from a single entry point.

We are currently in the process of finishing the texture reconstruction step and enhancing the complete framework. Thereafter, we will focus on validating our method in an ex-vivo setting. The accuracy of the 3D reconstruction can be assessed by using a 3D printed placenta model with fixed and known dimensions. Since, the introduction of foetal therapy in the Radboudumc in-vivo fetoscopic data is collected. This data will be used to test and optimize the algorithm on real fetoscopic images before it is applied during the FLOVA procedure. Much progress can be made by training the ORB-SLAM library on real fetoscopic images, in order to improve the feature detection and matching. Eventually, the 3D FLOVA-SLAM software will be implemented into the FLOVA procedure.

Ideally we would combine all our algorithms into one programming environment. Thereby, we aim to create a clear and simple interface of the software that can be used and controlled by the surgeon. The surgeon should be able to easily handle the camera calibration and the 3D reconstruction application. A standalone application will be built, so it can be rendered on any computer with enough computational power. In addition, attention will be paid to the visualization of the placental reconstruction during the FLOVA procedure in the operation room. The Radboudumc houses two hybrid operation rooms with endless visualization opportunities. This allows us to visualize the 3D reconstruction of the placenta in several ways, fully adapted to the preferences of the surgeon.

---

To enhance the visualization of the placenta even more, one could think about augmented reality (AR)<sup>62</sup>. AR can be used to align the real world, the patient and the uterus, with the virtual world, the placenta reconstruction. With AR it is possible to project the placenta reconstruction onto the patient. In the future it might even be possible to create an algorithm that detects the anastomoses and thereby displays the target vessels and an surgical planning on the placenta map. This could improve the safety and prevent surgical errors even more. However, literature on using AR based on reconstructed surface data in laparoscopic or endoscopic environments is limited<sup>93</sup>. In 2017, Mahmoud et al. was the first to publish ex-vivo results of using ORB-SLAM in combination with AR in endoscopy<sup>86</sup>. Nonetheless, the use of AR during in-vivo laparoscopy or endoscopy is hindered by the constantly deformable environment. Until this moment, there is no research into using AR for fetoscopic purposes. Although, the fetoscopic videos might have more potential for AR than laparoscopic videos, since there is less deformation during the surgery. Though, the coagulation of the placental vessels and the presence of two fetuses need to be accounted for.

Another possible application of the 3D FLOVA-SLAM software (in combination with AR) is objective fetoscopic training. The tracking function of the algorithm could potentially be used to calculate important parameters for the surgical performance, such as, time, path length and the motion smoothness. Objective training is already implemented into the field of laparoscopy<sup>94</sup>. For fetoscopy only a few objective training applications exist<sup>95,96,97</sup>. The advantage of using 3D FLOVA-SLAM, is the possibility to also assess the performances during the FLOVA procedure. In addition, our software could potentially be used in other medical specialisms our applications, i.e. in the field of cytoscopy or hysteroscopy.

In all foetal therapy centres worldwide, obstetricians face dilemmas related to the limited field of view and the diameter of the scope. The urgency to improve the field of view is reflected by the multiple publications relating this subject<sup>6,40,41</sup>. Therefore, we initiated the research project to investigate the possibility to integrate the 3D SLAM technique in the fetoscopy. The first results are promising, indicating that our approach has a high chance of success to address this urgent problem. The hypothesis is that, with the real-time map of the placenta, surgeons can use a smaller diameter during the procedure and hereby reduce the associated risks and complications, like pregnancy loss. Furthermore, we expect that a better orientation for the surgeon will lead to a faster procedure, shorter learning curves and improved accuracy leading to lower risk of complications (i.e. residual anastomoses). Ideally, a randomized controlled trial (RCT) will prove our hypothesis in the future.

---

## 4.9 Conclusion

The past year a framework for 3D FLOVA-SLAM has been developed, an application that can artificially expand the field of view during the FLOVA procedure. The application consists of five major steps. Small rod lens Hopkins fetoscopes are used for the image acquisition during the FLOVA procedure. Thereby, a special sterilisable calibration plate is developed in order to perform camera calibration inside the operating room. The 3D FLOVA-SLAM method is based on the recently developed ORB-SLAM, in combination with ORB feature extraction, and is used to generate a real-time 3D reconstruction of the placenta. Real-time texturing is added in order to provide the surgeon with an accurate representation of the placenta. The first results of using 3D FLOVA-SLAM on placental videos are promising, but more research is needed to finalize and optimize the software.

# Chapter 5

---

## *Conclusions and Recommendations*

---

After years of preparation, the Radboudumc finally started an IFTC in January 2018. With the introduction of foetal therapy, the Radboudumc houses the second IFTC of the Netherlands, providing care for the eastern part of the country. In addition, 3D FLOVA-SLAM has been developed, a software application to generate a real-time overview map of the placenta during FLOVA procedures.

Further work on this project should be focused on the expansion of the number of foetal therapy procedures, by implementing the FETO operation. In three years the minimal number of 20 foetal therapy procedures per year must be reached.

In addition, we plan to optimize and finish the 3D FLOVA-SLAM software. We hope that further tests will validate our method. Thereafter, the application can be implemented into the clinic. At last, we will carry out a clinical trial towards the added value of the 3D FLOVA-SLAM software for FLOVA procedures.

The last area for future research is the introduction of an accredited international school on foetal surgery, mainly focusing on the FLOVA procedure. In this way we are able to share our knowledge on using smaller instrumentation in combination with the 3D FLOVA-SLAM software. Hopefully, our methods and knowledge will lead to a reduction in foetal complications and an improvement of survival after FLOVA.

---

# Bibliography

- [1] F. Vandenbussche, D. Oepkes, L. Page-Christiaens, A. Go, J. Nijhuis, and A. Kwee. Quality Norm on Invasive Fetal Therapy. 2016.
- [2] M. Gaynor, F. Mostashari, and P. B. Ginsburg. Making health care markets work: Competition policy for health care. *JAMA*, 317(13):1313–1314, 2017.
- [3] M. Gandhi, R. Papanna, M. Teach, A. Johnson, and K. J. Moise. Suspected Twin-Twin Transfusion Syndrome: How often is the diagnosis correct and referral timely? *Journal of Ultrasound in Medicine*, 31(6):941–945, 2012.
- [4] R. Papanna, D. J. Biau, L. K. Mann, A. Johnson, and K. J. Moise. Use of the Learning Curve Cumulative Summation test for quantitative and individualized assessment of competency of a surgical procedure in obstetrics and gynecology: fetoscopic laser ablation as a model. *American Journal of Obstetrics and Gynecology*, 204(3):218, 2011.
- [5] S. H. P. Peeters, E. W. Van Zwet, D. Oepkes, E. Lopriore, F. J. Klumper, and J. M. Middeldorp. Learning curve for fetoscopic laser surgery using cumulative sum analysis. *Acta Obstetrica et Gynecologica Scandinavica*, 93(7):705–711, 2014.
- [6] V. Beck, P. Lewi, L. Gucciardo, and R. Devlieger. Preterm prelabor rupture of membranes and fetal survival after minimally invasive fetal surgery: A systematic review of the literature. *Fetal Diagnosis and Therapy*, 31(1):1–9, 2012.
- [7] L. Lewi, L. Gucciardo, T. Van Mieghem, P. de Koninck, V. Beck, H. Medek, D. Van Schoubroeck, R. Devlieger, L. De Catte, and J. Deprest. Monochorionic diamniotic twin pregnancies: natural history and risk stratification. *Fetal Diagnosis and Therapy*, 27(3):121–133, 2010.
- [8] N. J. Sebire, R. J. Snijders, K. Hughes, W. Sepulveda, and K. H. Nicolaides. The hidden mortality of monochorionic twin pregnancies. *British Journal of Obstetrics and Gynaecology*, 104(10):1203–1207, 1997.
- [9] L. L. Simpson. SMFM clinical guideline: Twin-twin transfusion syndrome. *American Journal of Obstetrics and Gynecology*, 208(1):3–18, 2013.
- [10] M. E. De Paepe and F. I. Luks. What-and why-the pathologist should know about twin-to-twin transfusion syndrome. *Pediatric and Developmental Pathology*, 16(4):237–51, 2013.
- [11] L. Lewi, J. Jani, I. Blickstein, A. Huber, L. Gucciardo, T. Van Mieghem, E. Doné, A. Boes, K. Hecher, E. Gratacós, P. Lewi, and J. Deprest. The outcome of monochorionic diamniotic twin gestations in the era of invasive fetal therapy: a prospective cohort study. *American Journal of Obstetrics and Gynecology*, 199(5):514, 2008.
- [12] R. Acosta-Rojas, J. Becker, B. Munoz-Abellana, C. Ruiz, E. Carreras, and E. Gratacos. Twin chorionicity and the risk of adverse perinatal outcome. *International Journal of Gynecology & Obstetrics*, 96(2):98–102, 2007.
- [13] E. Ortibus, E. Lopriore, J. Deprest, F. P. Vandenbussche, F. J. Walther, A. Diemert, K. Hecher, L. Lagae, P. De Cock, P. J. Lewi, and L. Lewi. The pregnancy and long-term neurodevelopmental outcome of monochorionic diamniotic twin gestations: a multicenter prospective cohort study from the first trimester onward. *American Journal of Obstetrics and Gynecology*, 200(5):494, 2009.
- [14] P. E. Weir, G. J. Ratten, and N. A. Beischer. Acute polyhydramnios - A complication of monozygous twin pregnancy. *BJOG: An International Journal of Obstetrics and Gynaecology*, 86(11):849–853, 1979.

- 
- [15] V. Berghella and M. Kaufmann. Natural history of twin-twin transfusion syndrome. *The Journal of reproductive medicine*, 46(5):480–484, 2001.
- [16] A. C. Rossi, D. Vanderbilt, and R. H. Chmait. Neurodevelopmental Outcomes After Laser Therapy for TwinTwin Transfusion Syndrome A Systematic Review and Meta-Analysis. *Obstetrics & Gynecology*, 118(5):1145–1150, 2011.
- [17] LUMC. FetusNed.
- [18] Michael Bebbington. Twin-to-twin transfusion syndrome: current understanding of pathophysiology, in-utero therapy and impact for future development. *Seminars in Fetal and Neonatal Medicine*, 15(1):15–20, 2010.
- [19] L. Lewi, J. Deprest, and K. Hecher. The vascular anastomoses in monochorionic twin pregnancies and their clinical consequences. *American Journal of Obstetrics and Gynecology*, 208(1):19–30, 2013.
- [20] R. A. Quintero, W. J. Morales, M. H. Allen, P. W. Bornick, P. K. Johnson, and M. Kruger. Staging of twin-twin transfusion syndrome. *Journal of Perinatology*, 19, 1999.
- [21] Nederlandse Vereniging voor Obstetrie en Gynaecologie. Richtlijn: Meerlingzwangerschap. Technical report, NVOG, 2011.
- [22] D. Roberts, J. P. Neilson, M. D. Kilby, and S. Gates. Interventions for the treatment of twin-twin transfusion syndrome. *The Cochrane database of systematic reviews*, 1(1), 2014.
- [23] M. V. Senat, J. Deprest, M. Boulvain, A. Paupe, N. Winer, and Y. Ville. Endoscopic Laser Surgery versus Serial Amnioreduction for Severe Twin-to-Twin Transfusion Syndrome. *The New England Journal of Medicine*, 351(2):136–144, 2004.
- [24] J. E. De Lia, D. P. Cruikshank, and W. R. Keye. Fetoscopic neodymium:YAG laser occlusion of placental vessels in severe twin-twin transfusion syndrome. *Obstetrics and gynecology*, 75(6):1046–1053, 1990.
- [25] R. A. Quintero, E. Kontopoulos, and R. H. Chmait. Laser Treatment of Twin-to-Twin Transfusion Syndrome. *Twin Research and Human Genetics*, 19(3):197–206, 2016.
- [26] J. D. De Lia, R. S. Kuhlmann, T. W. Harstad, and D. P. Cruikshank. Fetoscopic laser ablation of placental vessels in severe previable twin-twin transfusion syndrome. *American Journal of Obstetrics and Gynecology*, 172(4):1202–1211, 1995.
- [27] R. A. Quintero, W. J. Morales, G. Mendoza, M. Allen, C. S. Kalter, G. Giannina, and J. L. Angel. Selective photocoagulation of placental vessels in twin-twin transfusion syndrome: evolution of a surgical technique. *Obstetrical & gynecological survey*, 53(12):97–103, 1998.
- [28] R. A. Quintero, C. Comas, P. W. Bornick, M. H. Allen, and M. Kruger. Selective versus non-selective laser photocoagulation of placental vessels in twin-to-twin transfusion syndrome. *Ultrasound in Obstetrics and Gynecology*, 16(3):230–236, 2000.
- [29] R. A. Quintero, K. Ishii, R. H. Chmait, P. W. Bornick, M. H. Allen, and E. V. Kontopoulos. Sequential selective laser photocoagulation of communicating vessels in twintwin transfusion syndrome. *The Journal of Maternal-Fetal & Neonatal Medicine*, 20(10):763–768, 2007.
- [30] M. J. C. van Gemert, J. P. H. M. van den Wijngaard, E. Lopriore, L. Lewi, J. Deprest, and F. P. H. A. Vandebussche. Simulated Sequential Laser Therapy of Twin-Twin Transfusion Syndrome. *Placenta Journal*, 29(7):609–613, 2008.
- [31] Y. Ville, K. Hecher, A. Gagnon, N. Sebire, J. Hyett, and K. Nicolaides. Endoscopic laser coagulation in the management of severe twin-to-twin transfusion syndrome. *British journal of obstetrics and gynaecology*, 105(4):446–453, 1998.

- 
- [32] F. Slaghekke, E. Lopriore, L. Lewi, J. M. Middeldorp, E. W. Van Zwet, A. S. Weingertner, F. J. Klumper, P. DeKoninck, R. Devlieger, M. D. Kilby, M. A. Rustico, J. Deprest, R. Favre, and D. Oepkes. Fetoscopic laser coagulation of the vascular equator versus selective coagulation for twin-to-twin transfusion syndrome: An open-label randomised controlled trial. *The Lancet*, 383:2144–2151, 2014.
- [33] J. Akkermans, S. H. P. Peeters, F. J. Klumper, E. Lopriore, J. M. Middeldorp, and D. Oepkes. Twenty-Five Years of Fetoscopic Laser Coagulation in Twin-Twin Transfusion Syndrome: A Systematic Review. *Fetal Diagnosis and Therapy*, 38(4):241–253, 2015.
- [34] W. Diehl, A. Diemert, D. Grasso, S. Sehner, K. Wegscheider, and K. Hecher. Fetoscopic laser coagulation in 1020 pregnancies with twin-to-twin transfusion syndrome demonstrates improvement of double survival rates. *Ultrasound in Obstetrics & Gynecology*, 138(6):1328–1336, 2017.
- [35] J. Stirnemann, F. Djaafri, A. Kim, I. Mediouni, L. Bussieres, E. Spaggiari, C. Veluppillai, A. Lapillonne, E. Kermorvant, J. Magny, C. Colmant, and Y. Ville. Preterm premature rupture of membranes is a collateral effect of improvement in perinatal outcomes following fetoscopic coagulation of chorionic vessels for twin-twin transfusion syndrome: a retrospective observational study of 1092 cases. *BJOG: An International Journal of Obstetrics & Gynaecology*, 125(9):1154–1162, 2018.
- [36] J. Akkermans, S. H. P. Peeters, J. M. Middeldorp, F. J. Klumper, E. Lopriore, G. Ryan, and D. Oepkes. A worldwide survey of laser surgery for twin-twin transfusion syndrome. *Ultrasound in Obstetrics & Gynecology*, 45(2):168–174, 2015.
- [37] S. H. P. Peeters, J. Akkermans, M. Westra, E. Lopriore, J. M. Middeldorp, F. J. Klumper, L. Lewi, R. Devlieger, J. Deprest, E. V. Kontopoulos, R. Quintero, R. H. Chmait, J. S. Smoleniec, L. Otaño, and D. Oepkes. Identification of essential steps in laser procedure for twin-twin transfusion syndrome using the Delphi methodology: SILICONE study. *Ultrasound in Obstetrics and Gynecology*, 45(4):439–446, 2015.
- [38] A. J. Moon-Grady, A. Baschat, D. Cass, M. Choolani, J. A. Copel, T. M. Crombleholme, J. Deprest, S. P. Emery, M. I. Evans, F. I. Luks, M. E. Norton, G. Ryan, K. Tsao, R. Welch, and M. Harrison. Fetal Treatment 2017: The Evolution of Fetal Therapy Centers - A Joint Opinion from the International Fetal Medicine and Surgical Society (IFMSS) and the North American Fetal Therapy Network (NAFTNet). *Fetal Diagnosis and Therapy*, 42(4):241–248, 2017.
- [39] P. Klaritsch, K. Albert, T. Van Mieghem, L. Gucciardo, E. Done', B. Bynens, and J. Deprest. Instrumental requirements for minimal invasive fetal surgery. *BJOG: An International Journal of Obstetrics & Gynaecology*, 116(2):188–197, 2009.
- [40] S. G. Petersen, K. S. Gibbons, F. I. Luks, L. Lewi, A. Diemert, K. Hecher, J. E. Dickinson, J. J. Stirnemann, Y. Ville, R. Devlieger, G. Gardener, and J. A. Deprest. The Impact of Entry Technique and Access Diameter on Prelabour Rupture of Membranes Following Primary Fetoscopic Laser Treatment for Twin-Twin Transfusion Syndrome. *Fetal Diagnosis and Therapy*, 40(2):100–109, 2016.
- [41] R. Donepudi, J. Akkermans, L. Mann, F. J. Klumper, J. M. Middeldorp, E. Lopriore, K. J. Moise, M. Bebbington, A. Johnson, D. Oepkes, and R. Papanna. Recurrent Twin-Twin Transfusion Syndrome (rTTTS) and Twin Anemia Polycythemia Sequence (TAPS) after fetoscopic laser surgery (FLS): size (of the cannula) does matter. *Ultrasound in Obstetrics & Gynecology*, 2017.
- [42] J. Akkermans, L. van der Donk, S. H. P. Peeters, S. van Tuijl, J. M. Middeldorp, E. Lopriore, and Dick Oepkes. Impact of Laser Power and Firing Angle on Coagulation Efficiency in Laser Treatment for Twin-Twin Transfusion Syndrome: An ex vivo Placenta Study. *Fetal diagnosis and therapy*, 42(3):204–209, 2017.

- 
- [43] J. A. Deprest, D. Van Schoubroeck, P. P. Van Ballaer, H. Flageole, F. A. Van Assche, and K. Vandenberghe. Alternative technique for Nd : YAG laser coagulation in twin-to-twin transfusion syndrome with anterior placenta. *Ultrasound in Obstetrics and Gynecology*, 11(5):347–352, 1998.
- [44] J. M. Middeldorp, E. Lopriore, M. Sueters, F. W. Jansen, J. Ringers, F. J. C. M. Klumper, D. Oepkes, and F. P. H. A. Vandembussche. Laparoscopically guided uterine entry for fetoscopy in twin-to-twin transfusion syndrome with completely anterior placenta: A novel technique. *Fetal Diagnosis and Therapy*, 22(6):409–415, 2007.
- [45] Karl Storz Endoscopies. Every Detail Counts! Flexible Uretero-Renoscope Flex X2S: A New Dimension. Slender Design. Excellent Visualization., 2017.
- [46] E. B. Jelin, S. C. Schecter, K. D. Gonzales, S. Hirose, H. Lee, G. A. Machin, L. Rand, and V. A. Feldstein. Guide Wire Assisted Catheterization and Colored Dye Injection for Vascular Mapping of Monochorionic Twin Placentas. *Journal of Visualized Experiments*, (55):2837, 2011.
- [47] M. Reeff. *Mosaicing of endoscopic placenta images*. PhD thesis, ETH ZURICH, 2011.
- [48] P. Daga, D. I. Shakir, L. C. Garcia-peraza, M. Tella, G. Dwyer, A. L. David, J. Deprest, D. Stoyanov, T. Vercauteren, and S. Ourselin. Real-Time Mosaicing of Fetoscopic Videos using SIFT. *Medical Imaging 2016: Image-Guided Procedures, Robotic Interventions, and Modeling*, 9786:1–7, 2016.
- [49] S. Fransson. *Mosaicing of Fetoscopic Acquired Images using SIFT and FAST*. PhD thesis, KTH Royal Institute of Technology School of Computer Science and Communication, 2017.
- [50] H. Werner, J. L. Dos Santos, R. A. Sa, P. Daltro, E. Gasparetto, E. Marchiori, S. Campbell, and E. Araujo Junior. Visualisation of the vascular equator in twin-to-twin transfusion syndrome by virtual fetoscopy. *Archives of Gynecology and Obstetrics*, 292(6):1183–1184, 2015.
- [51] H. Liao, M. Tsuzuki, T. Mochizuki, E. Kobayashi, T. Chiba, and I. Sakuma. Fast image mapping of endoscopic image mosaics with three-dimensional ultrasound image for intrauterine fetal surgery. *Minimally Invasive Therapy and Allied Technologies*, 18(6):332–340, 2009.
- [52] L. Yang, J. Wang, E. Kobayashi, H. Liao, I. Sakuma, H. Yamashita, and T. Chiba. Ultrasound Image-Guided Mapping of Endoscopic Views on a 3D Placenta Model: A Tracker-Less Approach. *International Workshop on Medical Imaging and Virtual Reality Workshop on Augmented Environments for Computer-Assisted Interventions*, pages 107–116, 2013.
- [53] L. Yang, J. Wang, E. Kobayashi, T. Ando, H. Yamashita, I. Sakuma, and T. Chiba. Image mapping of untracked free-hand endoscopic views to an ultrasound image-constructed 3D placenta model. *The International Journal of Medical Robotics and Computer Assisted Surgery*, 11(2):223–234, 2015.
- [54] L. Yang, J. Wang, T. Ando, A. Kubota, H. Yamashita, I. Sakuma, T. Chiba, and E. Kobayashi. Self-contained image mapping of placental vasculature in 3D ultrasound-guided fetoscopy. *Surgical Endoscopy*, 30(9):4136–4149, 2016.
- [55] G. S. dos Santos, E. Maneas, D. Nikitichev, A. Barburas, A. L. David, J. Deprest, A. Desjardins, T. Vercauteren, and S. Ourselin. A Registration Approach to Endoscopic Laser Speckle Contrast Imaging for Intrauterine Visualisation of Placental Vessels. *International Conference on Medical Image Computing and Computer-Assisted Intervention*, pages 455–462, 2015.

- 
- [56] M. Tella, P. Daga, F. Chadebecq, S. Thompson, D. I. Shakir, G. Dwyer, R. Wimalasundera, J. Deprest, D. Stoyanov, T. Vercauteren, and S. Ourselin. A Combined em and Visual Tracking Probabilistic Model for Robust Mosaicking: Application to Fetoscopy. *IEEE Computer Society Conference on Computer Vision and Pattern Recognition Workshops*, pages 524–532, 2016.
- [57] F. Gaisser, S. H. P. Peeters, B. Lenseigne, P. P. Jonker, and D. Oepkes. Fetoscopic Panorama Reconstruction: Moving from Ex-vivo to In-vivo. *Annual Conference on Medical Image Understanding and Analysis*, pages 581–593, 2017.
- [58] C. Jeltès. Internship report: 2D Visual SLAM for artificial field of view expansion during fetal surgery. Technical report, Radboudumc, Nijmegen, 2017.
- [59] J. Deprest, G. Barki, Y. Ville, K. Hecher, E. Gratacos, and K. Nicolaides. Endoscopy in foetal medicine. Technical report, The EUROFOETUS and EuroTwin2Twin Group, 2004.
- [60] M. Yoshioka, Y. Maeda, and S. Omatu. Estimation of the optimal image resolution using the SIFT. In *The Fourteenth International Symposium on Artificial Life and Robotics*, 2009.
- [61] M. Reef, F. Gerhard, P. Cattin, and G. Székely. Mosaicing of Endoscopic Placenta Images, 2006.
- [62] B. Münzer, K. Schoeffmann, and L. Böszörmenyi. Content-based processing and analysis of endoscopic images and videos: A survey. *Multimedia Tools and Applications*, 77(1):1323–1362, 2018.
- [63] Z. Zhang. A Flexible New Technique for Camera Calibration. *IEEE Transactions on Pattern Analysis and Machine Intelligence*, 22(11):1330–1334, 2002.
- [64] J. Heikkilä. Geometric camera calibration using circular control points. *IEEE Transactions on Pattern Analysis and Machine Intelligence*, 22(10):1066–1077, 2000.
- [65] S. Thompson, Y. Meuer, E. Edwards, J. Ramalinho, M. R. Robu, D. Stoyanov, S. Ourselin, B. Davidson, D. Hawkes, and M. J. Clarkson. On pattern selection for laparoscope calibration. *Medical Imaging 2017: Image-Guided Procedures, Robotic Interventions, and Modeling*, 10135, 2017.
- [66] OpenCV. OpenCV, 1999.
- [67] J. Bouguet. Matlab camera calibration toolbox. *Caltech Technical Report*, 2000.
- [68] C. Wengert, M. Reef, P. Cattin, and G. Székely. Fully Automatic Endoscope Calibration for Intraoperative Use. pages 419–423, 2006.
- [69] Y. Hu, N. Yamanaka, and K. Masamune. Automatic Tracking Algorithm in Coaxial Near-Infrared Laser Ablation Endoscope for Fetus Surgery. *International Journal of Optomechatronics*, 8(3):159–178, 2014.
- [70] M.S. Nixon and A. S. Aguado. *Feature extraction & image processing for computer vision*. Academic Press, 3 edition, 2012.
- [71] D. G. Lowe. Distinctive Image Features from Scale-Invariant Keypoints. *International Journal of Computer Vision*, 60(2):91–110, 2004.
- [72] M.L. Groot Koerkamp. Internship report: Visual SLAM for artificial field of view expansion during fetal surgery. Technical report, University of Twente, 2016.
- [73] E. Rublee, W. Garage, and M. Park. ORB: an efficient alternative to SIFT or SURF. *2011 International Conference on Computer Vision*, pages 2564–2571, 2011.

- 
- [74] Floris Gaisser, Suzanne Peeters, Boris Lenseigne, Pieter Jonker, and Dick Oepkes. Stable Image Registration for In-Vivo Fetoscopic Panorama Reconstruction. *Journal of Imaging*, 4(1):24, 2018.
- [75] Ebrahim Karami, Siva Prasad, and Mohamed Shehata. Image Matching Using SIFT , SURF , BRIEF and ORB : Performance Comparison for Distorted Images. (February 2016), 2015.
- [76] T. Taketomi, H. Uchiyama, and S. Ikeda. Visual SLAM algorithms: a survey from 2010 to 2016. *IPSS Transactions on Computer Vision and Applications*, 9(1):16, 2017.
- [77] J. Engel, V. Koltun, and D. Cremers. Direct Sparse Odometry. *IEEE Transactions on Pattern Analysis and Machine Intelligence*, 40(3):611–625, 2016.
- [78] A. J. Davison, I. D. Reid, N. D. Molton, and O. Stasse. MonoSLAM: Real-Time Single Camera SLAM. *IEEE Transactions on Pattern Analysis and Machine Intelligence*, 29(6):1052–1067, 2007.
- [79] G. Klein and D. Murray. Parallel Tracking and Mapping for Small AR Workspaces. 2007.
- [80] R. Mur-Artal and J. D. Tardos. Fast Relocalisation and Loop Closing in Keyframe-Based SLAM. *2014 IEEE International Conference on Robotics and Automation (ICRA)*, 2014.
- [81] R. Mur-Artal and J. D. Tardos. ORB-SLAM2: An Open-Source SLAM System for Monocular, Stereo, and RGB-D Cameras. *IEEE Transactions on Robotics*, 33(5):1255–1262, 2017.
- [82] H. Strasdat, J. M. M. Montiel, and A. J. Davison. Visual SLAM: Why filter? *Image and Vision Computing*, 30(2):65–77, 2012.
- [83] B. Triggs, P. Mclauchlan, R. Hartley, and A. Fitzgibbon. Bundle Adjustment-A Modern Synthesis. *Lecture Notes in Computer Science*, pages 298–372, 2000.
- [84] G. Grisetti, R. Kümmerle, C. Stachniss, and W. Burgard. A Tutorial on Graph-Based SLAM. *IEEE Intelligent Transportation Systems Magazine*, 2(4):31–43, 2010.
- [85] M. Kazhdan, M. Bolitho, and H. Hoppe. Poisson Surface Reconstruction. In *Eurographics Symposium on Geometry Processing*, 2006.
- [86] N. Mahmoud, I. Cirauqui, A. Hostettler, C. Doignon, L. Soler, J. Marescaux, and J. M. M. Montiel. ORBSLAM-Based Endoscope Tracking and 3D Reconstruction. In *International Workshop on Computer-Assisted and Robotic Endoscopy*, pages 72–83. Springer, Cham, 2016.
- [87] N. Mahmoud, A. Hostettler, T. Collins, L. Soler, C. Doignon, and J. M. M. Montiel. SLAM based Quasi Dense Reconstruction For Minimally Invasive Surgery Scenes. In *ICRA 2017 workshop C4 Surgical Robots: Compliant, Continuum, Cognitive, and Collaborative*, 2017.
- [88] L. Qiu and H. Ren. Endoscope Navigation and 3D Reconstruction of Oral Cavity by Visual SLAM With Mitigated Data Scarcity. In *The IEEE Conference on Computer Vision and Pattern Recognition (CVPR) Workshops*, pages 2197–2204, 2018.
- [89] C. Cadena, L. Carlone, H. Carrillo, Y. Latif, D. Scaramuzza, J. Neira, Ian Reid, and John J. Leonard. Past, present, and future of simultaneous localization and mapping: Toward the robust-perception age. *IEEE Transactions on Robotics*, 32(6):1309–1332, 2016.
- [90] K. L. Lurie, R. Angst, D. V. Zlatev, J. C. Liao, and A. K. Ellerbee Bowden. 3D reconstruction of cystoscopy videos for comprehensive bladder records. *Biomedical Optics express*, 8(4):2106–2123, 2017.
- [91] P. A. Foteinos, A. N. Chernikov, and N. P. Chrisochoides. Guaranteed quality tetrahedral Delaunay meshing for medical images. *Computational Geometry*, 47(4):539–562, 2014.

- 
- [92] A. Fedorov, N. Chrisochoides, R. Kikinis, and S. Warfield. Tetrahedral Mesh Generation for Medical Imaging. Technical report, 2012.
- [93] L. Maier-Hein, P. Mountney, A. Bartoli, H. Elhawary, D. Elson, A. Groch, A. Kolb, M. Rodrigues, J. Sorger, S. Speidel, and D. Stoyanov. Optical techniques for 3D surface reconstruction in computer-assisted laparoscopic surgery. *Medical Image Analysis*, 17:974–996, 2013.
- [94] J. L. Emken, E. M. McDougall, and R. V. Clayman. Training and assessment of laparoscopic skills. *JSLIS : Journal of the Society of Laparoendoscopic Surgeons*, 8(2):195–199, 2004.
- [95] T. Wataganara, A. Gosavi, K. Nawapun, P. D. Vijayakumar, N. Phithakwatchara, M. Choolani, L. L. Su, A. Biswas, and C. N. Z. Mattar. Model Surgical Training: Skills Acquisition in Fetoscopic Laser Photocoagulation of Monochorionic Diamniotic Twin Placenta Using Realistic Simulators. *Journal of Visualized Experiments*, (133):57328–57328, 2018.
- [96] S. H. P. Peeters, J. Akkermans, J. Bustraan, J. M. Middeldorp, E. Lopriore, R. Devlieger, L. Lewi, J. Deprest, and D. Oepkes. Operator competence in fetoscopic laser surgery for twin-twin transfusion syndrome: validation of a procedure-specific evaluation tool. *Ultrasound in Obstetrics & Gynecology*, 47(3):350–355, 2016.
- [97] S. H. P. Peeters, J. Akkermans, F. Slaghekke, J. Bustraan, E. Lopriore, M. C. Haak, J. M. Middeldorp, F. J. Klumper, L. Lewi, R. Devlieger, L. De Catte, J. Deprest, S. Ek, M. Kublickas, P. Lindgren, E. Tiblad, and D. Oepkes. Simulator training in fetoscopic laser surgery for twin-twin transfusion syndrome: a pilot randomized controlled trial. *Ultrasound in Obstetrics & Gynecology*, 46(3):319–326, 2015.



# Chapter 6

---

## *Appendices*

6.1	Appendix A: Calibration Protocol . . .	84
6.2	Appendix B: Calibration Method . . .	86
6.3	Appendix C: ORB Feature Extraction	88
6.4	Appendix D: ORB-SLAM . . . . .	90

---

## 6.1 Appendix A: Calibration Protocol

**Introductie** Vanwege het gelimiteerde gezichtsveld van de fetoscoop, wordt er gekeken naar een manier om de placenta beter in beeld te brengen. Het doel is om een Google Maps-achtige techniek te ontwikkelen die de vasculaire topografie van het placentaoppervlak in kaart kan brengen. Deze techniek combineert alle door de operateur geziene videobeelden tot een complete landkaart zichtbaar op het scherm, op basis waarvan de operateur weloverwogen keuzes kan maken.

Optische vervormingen van de fetoscopische beelden hebben een averechts effect op het combineren van de videobeelden. Daarom is het belangrijk om voor deze vervormingen te corrigeren en de fetoscoop perioperatief te kalibreren. Omdat de fetoscoop zich tijdens de interventie in het vruchtwater bevindt, en de refractie index in vloeistof verschilt van lucht, is een klassieke kalibratie methode niet mogelijk. Bovendien is een perioperatieve fetoscopische camerakalibratie in vloeistof onpraktisch vanwege sterilisatievereisten en beperkingen van de materialen die in de operatiekamer zijn toegestaan.

Daarom is er een methode ontwikkeld om praktisch en steriel de camera te kalibreren met een patroon van cirkels en twee rechthoeken. Deze methode maakt gebruik van een aangepast algoritme van Wengert et al. en een speciaal ontwikkeld kalibratieplaatje van RVS.

### Materialen

- Steriel kalibratiebord
- Steriele container
- Demi water
- Laptop/computer met Debut Video Capture Software
- Hopkins fetoscoop
- Karl Storz endoscopie toren

---

## Protocol

1. Fetoscopische video acquisitie
  - (a) Plaats het kalibratiebord in een steriele container
  - (b) Vul de container met de gewenste steriele vloeistof Opmerking: Tijdens fetoscopische procedures is dit eigenlijk vruchtwater. Aangezien NaCl vergelijkbare optische eigenschappen heeft als vruchtwater, kan steriel saline water worden gebruikt voor de kalibratie van de fetoscoop
  - (c) Pas de zoom en de resolutie van de fetoscoop aan. (Let op, met deze parameters moet ook de procedure worden uitgevoerd!)
  - (d) Voor witbalans uit
  - (e) Breng de fetoscoop in de vloeistof en houd deze op een afstand van de het kalibratiebord vergelijkbaar met de afstand die wordt gebruikt bij de latere procedure
  - (f) Sluit de scopie-toren aan op de research laptop
  - (g) Start het programma Debut Professional
  - (h) Beweeg de tip van de fetoscoop langzaam voor verschillende weergaven terwijl de twee rechthoekjes altijd in beeld blijven. Zorg ervoor dat deze rechthoeken ongeveer in het midden van het beeld zitten voor optimale prestaties
  - (i) Maak van elke weergave een opname met het programma Debut. Zorg voor tenminste 10 frames (idealerweise tussen de 10 en 20).

## Referenties

1. Wengert, C., Reeff, M., Cattin, P. C., & Szkely, G. (2006). Fully automatic endoscope calibration for intraoperative use. In *Bildverarbeitung für die Medizin 2006* (pp. 419-423). Springer, Berlin, Heidelberg.
2. Reeff M., Gerhard F., Cattin P.C., Szkely G., Mosaicing of endoscopic placenta images. Citeseer; 2011.
3. Steigman S.A., Kunisaki S.M., Wilkins-Haug L., Takoudes T.C., Fauza D.O., Optical properties of human amniotic fluid: implications for videofetoscopic surgery. *Fetal diagnosis and therapy*. 2009;27(2):8790.

---

## 6.2 Appendix B: Calibration Method

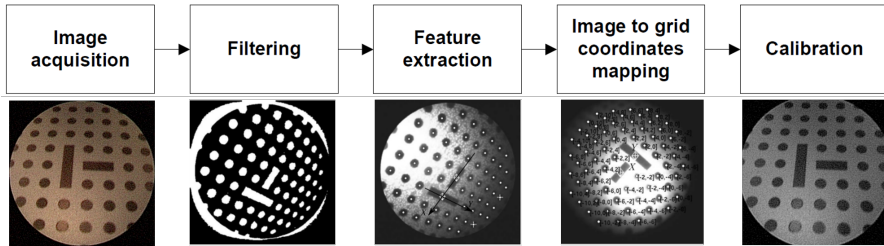


Figure 6.1 Overview of the five-step camera calibration algorithm.

**Filtering** The calibration algorithm starts with converting the coloured images into grey scale images. Then a threshold is applied to create a binary image. Because of the varying illumination throughout the images, Gaussian adaptive thresholding is used. By calculating different thresholds for different regions we can overcome the problems of different lighting conditions in different areas of the image. After applying the threshold, we reduce the impulse noise by the use of a median filter. At last, morphological closing is performed to close the white dots in the image.

**Feature extraction** Subsequently, the features (white dots) are extracted using connected component analysis. Every blob is characterized by a number of parameters like the ellipticity, solidity, orientation and area. The centre of gravity of the blobs serves as grid point location. All wrongly created blobs are excluded based on the characteristics, i.e. to large or to small area. The rectangular orientation marks are recognized by their ellipticity and area. The centre of gravity of the largest orientation marker is taken as the origin of the coordinate system. Images are discarded when the orientation markers are not or wrongly detected.

**Image to grid coordinates mapping** The found image coordinates of the grid points need to be matched with the grid coordinates. This is done by searching every grid point from the centre of the image outwards. The algorithm starts with the x-axis. From point  $x_0$  the nearest grid point is sought in a given radius in the positive direction. When the grid point is found the following grid point is sought using an adapted radius. When no grid points are found in that direction, the procedure is followed by searching in the negative direction. Then the algorithm continues by searching on the y-axis. The algorithm ends by searching for all the grid points on the lines parallel to the y-axis. When all the grid points are matched

---

to the grid coordinates a transformation matrix is computed. The reprojection error is used to discard images in which the matching of the image coordinates with the grid coordinates failed.

At last, the calibration parameters are calculated using the Bouguets Camera Calibration Toolbox.

## References

1. M. Reeff. Mosaicing of endoscopic placenta images. PhD thesis, ETH ZURICH, 2011.
2. J. Bouguet. Matlab camera calibration toolbox. Caltech Technical Report, 2000.

---

## 6.3 Appendix C: ORB Feature Extraction

Oriented FAST and Rotated BRIEF (ORB) is a local feature detection method which was first presented by Rublee et al. in 2011. ORB is based on the Features from accelerated Segment Test (FAST) keypoint detector and the visual descriptor Binary Robust Independent Elementary Feature (BRIEF).

**Detection** The FAST detector is a computational efficient corner detection method. The FAST detector uses a Bresenham circle (radius 3) to indicate the corners. Every pixel (x,y) is being compared to the 16 surrounding pixels based on their intensities (I). If a N-number of contiguous pixels all have a higher intensity than the pixel (x,y) plus a threshold t, the pixel is indicated as a feature. This also implies if all surrounding pixels have lower intensities. With the FAST method the orientations of the features are not computed. To make ORB rotational invariant a modification of FAST was made. For every feature/corner, the intensity weighted centroid of the surrounding patch is calculated. The orientation is determined as the direction of the vector from the feature to the centroid. Besides, FAST is also not scale invariant. In ORB this is handled by employing a scale image pyramid in order to produce multi-scale features. At the end a Harris corner measure is used to find the top N features in the image.

**Description** ORB uses the highly efficient BRIEF descriptor for the feature description. For each feature a square patch around it is drawn and then smoothed using a Gaussian kernel. For every patch a binary vector is computed wherein each bit is calculated by comparing the intensity of two pixels of the patch.

The BRIEF descriptor is not scale or rotation invariant. An adaptation of BRIEF was made in order to make it invariant to in-plane rotations. This is done by steering BRIEF using the orientation of the keypoints. Furthermore, a learning method was developed in order to

**Matching** Features can be matched in various ways. In our model the features are matched using the bag-of-words (BoW) model. In document classification a codeword is analogue to words in a text document. In computer vision, the BoW model is used to classify image features and treat them as words.

After the image features are described as a binary string, the BoW model converts these string-represented patches into codewords using k-medians clustering. A codeword represents a cluster of similar patches. All codewords together form

---

a codebook. The codebook is structured in a hierarchical way as a tree. This structure is used to perform a targeted search between features of comparable image frames. When a possible match is found, the Hamming distance is used for geometrical validation. The Hamming distance measures the distance between two strings by determining the amount of different bits between them. This distance can be calculated much more efficient, than the frequently used Euclidean distance, as used in SIFT. If the obtained Hamming distance between two descriptors is less than a chosen threshold, the descriptors are matched. In addition, RANSAC is used to exclude wrongly matched feature pairs.

## References

1. E. Rublee, W. Garage, and M. Park. ORB: an efficient alternative to SIFT or SURF. 2011 International Conference on Computer Vision, pages 2564-2571, 2011.

---

## 6.4 Appendix D: ORB-SLAM

The complete ORB-SLAM method exists of 3 main components which are runned in parallel: tracking, local mapping and loop detection (figure 6.2).

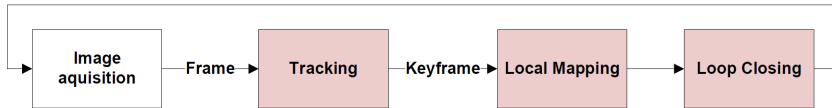


**Figure 6.2** Overview of the complete ORB-SLAM method. The ORB-SLAM method exists of three main components which are runned in parallel: tracking, local mapping and loop detection.

**Tracking** The tracking thread (figure 6.3) deals with every acquired image frame from the camera. This process starts with extracting ORB features in an image frame. Then the initial camera pose is predicted. When the tracking was successful for the last frame, the initial camera pose is calculated using a constant velocity motion model. Subsequently, the pose is optimized by matching the features of the previous frame with the features of the current frame. If the tracking was not successful for the last frame, relocalization of the camera is necessary. This is done by place recognition. All features that are found in the frame are converted into a visual vocabulary using the Bag of Words method. Thereafter, the recognition database searches for keyframe candidates with a comparable camera pose as in the current frame using the PnP algorithm. The camera pose is optimized by searching feature matches between the keyframe and the current frame. With the estimation of the camera position and the initial set of feature matches the map is projected onto the frame. Consequently more feature matches are searched and the camera pose is finally optimized. The last step of the tracking thread is to decide whether the current frame can be used as a keyframe. A keyframe is inserted when multiple conditions are met. More details about this conditions can be found in the original ORB-SLAM article.

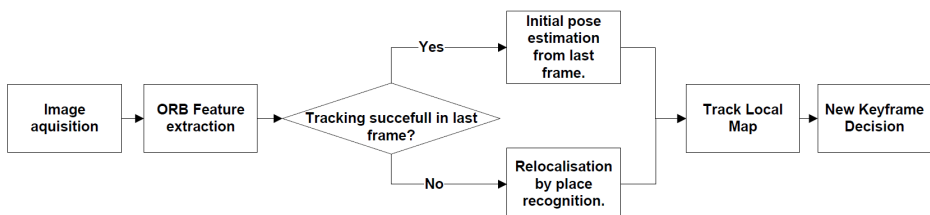


**Figure 6.3** Overview of the ORB-SLAM tracking function.

---

**Local mapping** The local mapping thread (figure 6.4) handles the new keyframes that are selected in the tracking part. When the new keyframe is inserted, the co-visibility graph and the visual vocabulary are updated. The local mapping thread also handles the removal and insertion of the map points. Wrongly matched or not trackable points are removed. New map points are created in the current keyframe by triangulating ORB feature matches from connected keyframes in the co-visibility graph. Local bundle adjustment is used to optimize the current keyframe, all keyframes connected in the co-visibility graph, all the map points seen from this keyframe and all keyframes that see those points but are not connected. At last, redundant keyframes are detected and deleted.

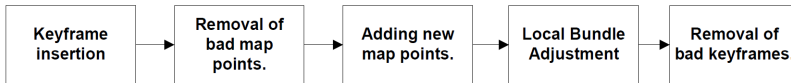


**Figure 6.4** Overview of the ORB-SLAM local mapping function.

**Loop closing** The loop closing thread (figure 6.5) handles the just processed keyframes and tries to detect and close loops. The current keyframe is compared to neighbours in the co-visibility graph using the visual vocabulary. The keyframe with the best correspondence to the current frame is selected. Keyframes which directly connect to the current keyframe are not taken into account. When the correspondence between the keyframes is found in three consecutive frames, a possible loop is detected. Subsequently, a similarity transformation is performed between the two keyframes. When enough feature matches are found, the loop is accepted and fused. Duplicated map points are fused, the co-visibility graph is updated and all involved keyframes are corrected using the similarity transformation. At last, a pose graph optimization is performed as described in the tracking part.

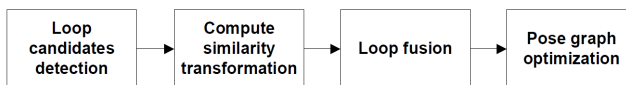


**Figure 6.5** Overview of the ORB-SLAM loop closing function.

---

## References

1. R. Mur-Artal and J. D. Tardos. Fast Relocalisation and Loop Closing in Keyframe-Based SLAM. 2014 IEEE International Conference on Robotics and Automation (ICRA), 2014.
2. R. Mur-Artal and J. D. Tardos. ORB-SLAM2: An Open-Source SLAM System for Monocular, Stereo, and RGB-D Cameras. *IEEE Transactions on Robotics*, 33(5):1255-1262, 2017.

The twin-twin transfusion syndrome (TTTS) occurs in 20% of the monochorionic pregnancies and results from unbalanced foeto-foetal blood transfusion between the donor twin and the recipient twin through placental anastomoses. Fetoscopic laser occlusion of vascular anastomoses (FLOVA) is commonly used to treat the underlying pathology of TTTS. During this procedure the anastomoses are identified and coagulated using a small fetoscope. In this way the two foetal circulations will become separated and blood transfusions cannot longer occur. In the Netherlands the referral hospital for patients with TTTS is the Leiden University Medical Center (LUMC). Although, FLOVA is commonly used in the field of foetal therapy, it is characterized by the disadvantage of a small field of view during the procedure. This can lead to a difficulty in orientation and navigation for the surgeon.

The first objective of this research was to implement FLOVA in the Radboudumc and to create the second invasive foetal therapy centre of the Netherlands. The second aim of this project was to overcome the problems of the limited field of view during FLOVA by implementing a method that can provide a real-time 3D overview map of the placental vascular topography. This map can help the surgeon orientate and navigate during the FLOVA procedures, potentially improving the accuracy and thereby reducing the chance of complications, the operation time and the costs.

Years of preparation, were followed by the introduction of the FLOVA procedure in the Radboudumc in January this year. Hereby, the Radboud now is the referral centre for the eastern part of the Netherlands. In May the first FLOVA operation was successfully performed. Furthermore, a framework for the 3D FLOVA-SLAM software has been developed. 3D FLOVA-SLAM is based on the recently developed ORB-SLAM and is used to generate a real-time textured 3D reconstruction of the placenta. The 3D FLOVA-SLAM method can be used without external hardware. The first results of using 3D FLOVA-SLAM on placental videos are promising, indicating that our approach has a high chance of success to address the urgent problem of the limited field of view during FLOVA procedures.

The hypothesis is that, with the real-time map of the placenta, surgeons can use smaller diameter instruments during the procedure and hereby reduce the associated risks and complications, like pregnancy loss. Furthermore, we expect that a better orientation for the surgeon will lead to a faster procedure, shorter learning curves and improved accuracy leading to lower risk of complications.